AD-A128 241 ACTUATOR-PLACEMENT CONSIDERATIONS FOR THE CONTROL OF LARGE SPACE STRUCTURES(U) NAVAL RESEARCH LAB WASHINGTON DC R E LINDBERG 11 MAY 83 NRL-8675 1/1

UNCLASSIFIED F/G 22/1 NL

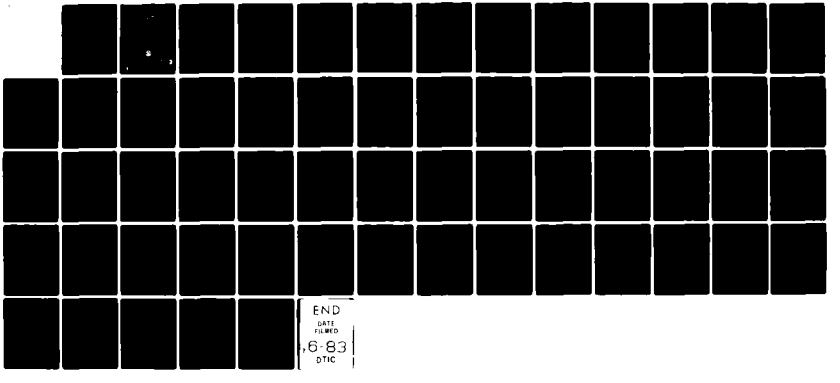

END
DATE FILMED
6-83
DTIC

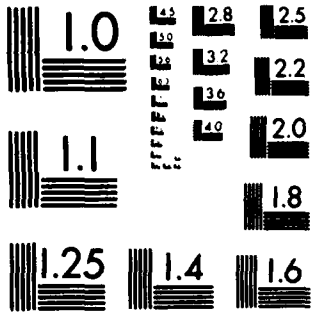

NRL Report 8675

Actuator-Placement Considerations for the Control of Large Space Structures

ROBERT E. LINDBERG, JR.

Advanced Systems Branch
Aerospace Systems Division

May 11, 1983

NAVAL RESEARCH LABORATORY
Washington, D.C.

SECURITY CLASSIFICATION OF THIS PAGE (When Data Entered)

REPORT DOCUMENTATION PAGE		READ INSTRUCTIONS BEFORE COMPLETING FORM
1. REPORT NUMBER NRL Report 8675	2. GOVT ACCESSION NO.	3. RECIPIENT'S CATALOG NUMBER
4. TITLE (and Subtitle) ACTUATOR-PLACEMENT CONSIDERATIONS FOR THE CONTROL OF LARGE SPACE STRUCTURES		5. TYPE OF REPORT & PERIOD COVERED Final report on one phase of a continuing problem. 6. PERFORMING ORG. REPORT NUMBER
7. AUTHOR(s) Robert E. Lindberg, Jr.		8. CONTRACT OR GRANT NUMBER(s)
9. PERFORMING ORGANIZATION NAME AND ADDRESS Naval Research Laboratory Washington, DC 20375		10. PROGRAM ELEMENT, PROJECT, TASK AREA & WORK UNIT NUMBERS 61153N RR014-02-41 79-0713-0
11. CONTROLLING OFFICE NAME AND ADDRESS Office of Naval Research Arlington, VA 22217		12. REPORT DATE May 11, 1983 13. NUMBER OF PAGES 58
14. MONITORING AGENCY NAME & ADDRESS(if different from Controlling Office)		15. SECURITY CLASS. (of this report) UNCLASSIFIED 15a. DECLASSIFICATION/DOWNGRADING SCHEDULE

16. DISTRIBUTION STATEMENT (of this Report)

Approved for public release, distribution unlimited.

17. DISTRIBUTION STATEMENT (of the abstract entered in Block 20, if different from Report)

18. SUPPLEMENTARY NOTES

19. KEY WORDS (Continue on reverse side if necessary and identify by block number)

Large space structures	Controllability
Flexible satellite control	Optimal control
Actuator placement	Degree of controllability
Distributed parameter systems	Independent modal space control

20. ABSTRACT (Continue on reverse side if necessary and identify by block number)

Actuator placement for the control of distributed-parameter systems such as large flexible space structures is considered in detail. The first focus is on the degree of controllability as defined in a previous work. Its behavior and approximation is considered via simple problems for which the exact value may be computed. The upper-bound approximation is found to be periodically exact for harmonic systems and acceptable for lightly damped systems. A method is proposed for avoiding the unacceptable behavior of the approximation when a problem has nearly repeated roots.

(Continued)

DD FORM 1 JAN 73 1473 EDITION OF 1 NOV 65 IS OBSOLETE
S/N 0102-014-6601

SECURITY CLASSIFICATION OF THIS PAGE (When Data Entered)

20. ABSTRACT (Continued)

Because the upper-bound approximation in the problem of a double-integral plant diverges, a new lower-bound approximation is developed based on discretization of the continuous-time system.

The approximate degree of controllability in three forms (for time-optimal, energy-optimal, or fuel-optimal control policy) is applied to the problem of optimal actuator placement for control of transverse oscillation of a simply supported beam. Both predictable and unanticipated optimal solutions are encountered. The concept of a degree of control spillover is then developed, motivated by the limited fidelity inherent in structural models. A composite criterion incorporating both degree of controllability and degree of control spillover is again applied to the simply-supported-beam problem.

Design freedom involving number and placement of actuators is next examined for the computationally simple Independent Modal Space Control (IMSC) design method. A new formulation of IMSC eliminates the fundamental restriction of previous work that one actuator is required for each mode to be controlled. This enhancement allows the design of linear-quadratic optimal controls for extremely large dimensional systems. Actuator placement is then of prime importance in physically realizing the optimal control laws. Methods for actuator-placement optimization are developed for use with ISMC. The methods are computationally comparatively simple and separate the actuator-placement task from the control-law design, a unique feature of this approach.

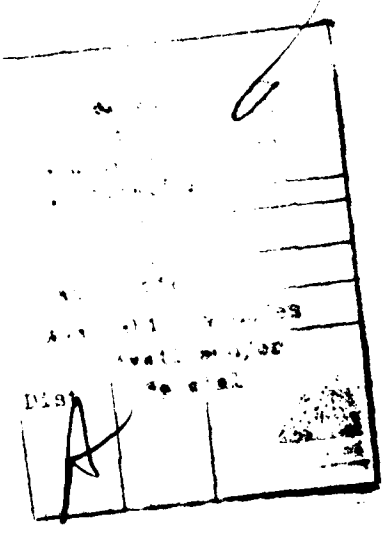

CONTENTS

This work is a revised version of the author's doctoral dissertation
in mechanical engineering at Columbia University.

ACTUATOR-PLACEMENT CONSIDERATIONS FOR THE CONTROL OF LARGE SPACE STRUCTURES

1. INTRODUCTION

1.1 Overview

The control of distributed-parameter systems (that is, systems most appropriately modeled by partial differential equations) is an area of research which requires extensions to the established control theory which has been developed for application to lumped-parameter systems (the dynamics of which are conventionally described by ordinary differential equations). The motivation for much recent work in this area has been the problem of control of large space structures.

In the field of satellite design, the complexity of control systems has evolved rapidly. Most small earth-pointing satellites require only relatively simple attitude-stabilization systems which rely on techniques such as spin stabilization, dual-spin stabilization, and gravity-gradient stabilization. The active attitude control of satellites requiring precise pointing and maneuvering is accomplished by more complex attitude-control systems involving reaction wheels, control moment gyros (CMGs), magnetic torquers, or gas thrusters. Both types of satellites are typically treated as rigid bodies, and the control systems are successfully developed using either classical or modern control techniques by designing the systems based on the equations which describe the satellite's rigid-body dynamics.

Beyond the capabilities of this technology lies the problem of controlling spacecraft attitude in the presence of structural flexibility. The capability and desire to place satellites of ever larger dimension in space while minimizing on-orbit mass will lead to spacecraft structural designs which are pervasively flexible. Control systems for such spacecraft must, at the very least, account for the perturbations in attitude induced by structural vibration. If, in addition, the structural deformations affect the mission performance (such as deformations in antennas or optical support structures), then the attitude control will be necessarily coupled with the additional problem of shape control. It is this complex composite control problem which is the motivation of the work presented herein.

There are several characteristics of the problem of controlling large flexible spacecraft which distinguish it from the standard attitude-control problem. The dynamics of the structural deformations would be most appropriately described by partial differential equations involving independent variables in both time and space. For complex systems, however, partial-differential-equation models are seldom achievable; in addition, the bulk of modern and optimal control theory assumes a discrete-plant model. For these reasons, the dynamics of flexible spacecraft are typically approximated by a system of coupled ordinary differential equations in time, whose dependent variables are generalized spatial coordinates. If modal coordinates are chosen, then the ordinary differential equations describe the orthogonal modes of vibration of the system.

This approach to approximating the system dynamics by a finite number of modes implicitly acknowledges that a portion of the dynamics, often associated with higher frequency modes of vibration, has been truncated from the model. The problem of model truncation and the design of a control based on a truncated model is the first characteristic which distinguishes this problem from the conventional attitude-control problem.

Manuscript approved November 19, 1982.

Another property of flexible-structure control systems is that the actuator placement impacts the control design. The control of a rigid structure is, in many cases, theoretically independent of the location of the actuators which provide the control action. In contrast, when it is important to achieve shape control, the actuator placement on the structure to effectively provide that control is a primary design consideration.

In this work, the problem of actuator-placement optimization is treated in detail. Several alternative optimization criteria will be considered, each reflecting some measure of the controllability of the system as a function of actuator locations. In addition, the impact of model truncation on the actuator-placement problem is considered.

1.2 Background

The concept of controllability of a mathematical model of a physical system is one of the fundamental results of modern control theory and is an important tool in the design of control systems. As originally introduced by Kalman,[1] the check for complete controllability via the well-known rank test on the controllability matrix provides an answer to the *binary* question of whether or not a system is completely controllable.

In stability theory, it is often important to know not only whether a system is stable or unstable but also how stable. It follows, then, that a quantitative rather than qualitative measure of controllability also would be a useful design aid. The questions to be answered are "how controllable is the system?," "which configuration is *more* controllable?," or ultimately "which among the class of all completely controllable systems is the *most* controllable?"

These questions were first addressed in an early study by Kalman, Ho, and Narendra,[2] who proposed a weighted trace of the controllability Gramian as a controllability measure. Brown[3] and Monzingo[4] addressed the question of relative observability of linear systems (and implied the treatment of controllability via duality). They recognized that the relationship between the column vectors of the observability matrix can identify the least observable direction in the state space. Johnson[5] extended the work of Kalman, Ho, and Narendra, considering in particular the trace and determinant of the inverse controllability Gramian as scalar measures of controllability. Müller and Weber[6] identified the maximum eigenvalue, trace, and determinant of the inverse controllability Gramian as three special cases of a more general form of scalar controllability measure dependent on an independent parameter. Variation of that parameter leads to an infinite set of scalar measures of relative controllability, any of which could be used, for instance, in optimizing actuator placement. Friedland[7] defined a controllability index based on the conditioning number of the controllability matrix. This index was shown to be independent of state normalization.

A common thread binds all of these developments, in that the proposed quantitative measures of controllability are based on information inherent in either the controllability matrix or the controllability Gramian. Each leads to a measure which may be associated with the minimum energy or average energy required to control the particular system. Optimization based on such a measure therefore implicitly assumes the use of a minimum energy control. An entirely new approach was presented recently by Viswanathan, Longman, and Likins[8] and Viswanathan,[9] who proposed a scalar measure based on the set of recoverable states associated with a specified recovery time T. This degree of controllability is developed by considering the time-optimal regulator problem. The results were extended by Viswanathan and Longman[10] to handle systems with repeated roots and by Longman and Alfriend[11] to treat the time-optimal tracking problem.

The balance of this section summarizes the development of the degree of controllability as defined by Viswanathan, Longman, and Likins and methods for its approximation as presented in Refs. 8 and 9.

Section 2 investigates several aspects of the degree of controllability by considering simple systems for which the exact value of the degree of controllability is readily obtained. In this way, the behavior of the proposed methods of approximation are critically examined.

The results of section 2 motivate the development of a new conservative (lower-bound) approximation to the degree of controllability. This new approximation method, based on discretization of the continuous system, is presented in section 3.

The optimization of actuator locations for the control of transverse oscillation of a simple flexible structure is detailed in section 4. The effects of model fidelity and system normalization are considered for various forms of the degree of controllability, resulting in both predictable and unanticipated results.

The concern regarding the effects of model truncation, in conjunction with the simple, not necessarily satisfactory, nature of the optimal actuator placement for control of free-free structures leads to the development of ε quantity termed the degree of control spillover. The definition of this new concept and methods for its approximation are presented in section 5. A new composite criterion for actuator-placement optimization is then proposed, which reflects the desirability of both effectively controlling the system modes included in the model and limiting the excitation of known residual modes.

The various forms of the degree of controllability implicitly assume that the associated control laws will be obtained by conventional optimal-control techniques (specifically time-optimal, energy-optimal, or fuel-optimal control). Recently a new control-design technique has been developed and shown to be particularly attractive computationally for systems described by a large number of ordinary differential equations. The technique, known as Independent Modal Space Control, obtains optimal control laws which are independent of actuator locations. The fundamental limitation of the approach is that heretofore the technique has required one actuator for each mode included in the system dynamics. In section 6, this design technique is critically examined, and a new formulation is presented which eliminates the restriction on the number of actuators required. The problem of actuator-placement optimization is then addressed, and simple open-loop and closed-loop criteria are formulated.

The principal contributions of this work to the field of large-space-structure control in general and the problem of actuator-placement optimization in particular are summarized in the conclusion, section 7.

1.3 Degree of Controllability

The system under consideration is that of the linear time-invariant regulator problem with bounded measurable controls. In terms of the normalized state vector x and the normalized control vector u, the system may be expressed as

$$\dot{x}(t) = Ax(t) + Bu(t), \tag{1}$$

with

$$|u_i(t)| \leqslant 1, \quad i = 1, 2, \ldots, m. \tag{2}$$

The control objective of a regulator control is to drive the state to $x = 0$. A normalization of the state vector accomplishes the task of specifying the relative importance of driving each state element $x_i(t)$, $i = 1, 2, \ldots, n$, to zero.

For this system, the degree of controllability as developed by Viswanathan, Longman, and Likins[8] is based upon the following definitions:

Definition 1. The *recovery region for time* T for the normalized system described by Eqs. (1) and (2) is the set

$$R = \{x(0) \mid \exists\, u(t),\ t \in [0,T],\ |u_i(t)| \leqslant 1 \text{ for } i = 1,2,\ \ldots,\ m,\ \ni\ x(T) = 0\}.$$

Definition 2. The *degree of controllability in time* T *of the* x = 0 *solution* of the normalized system described by Eqs. (1) and (2) is defined as

$$\rho = \inf ||x(0)|| \ \forall\ x(0) \notin R,$$

where $||\ldots||$ represents the Euclidean norm.

The degree of controllability for time T is thus a scalar measure of the size of the recovery region, taken as the infimal distance from the origin to the set of initial states which cannot be returned to the origin in time T. Several remarks may be made regarding the implications of the above definitions:

- Time-optimal control of the system is implied, since the boundary of the recovery region is the locus of all states which can be returned to the origin using minimum time control;
- The previously mentioned normalization of the state will have an important influence on the degree of controllability, since the norm of the state vector depends on that normalization;
- When the system described by Eq. (1) is uncontrollable in the binary sense, the recovery region for any time T will have dimension less than that of the state space; therefore the degree of controllability will be zero.

The last remark is intuitively pleasing and was, in fact, established as a prerequisite for the development of the definition of degree of controllability.[8]

Upon introduction of this definition of degree of controllability, Viswanathan, Longman, and Likins[8] subsequently addressed the problem of approximating the recovery region and obtained a general form for an approximate degree of controllability. The procedure involves choosing a set of n linearly independent directions in the state space and constructing a parallelepiped with sides parallel to these directions such that there is some point on each side which is in the recovery region but such that no point outside the parallelepiped lies inside the recovery region. The minimum among the perpendicular distances to the sides of the parallelepiped is then taken as an approximation to the degree of controllability.

Any linearly independent spanning set (for example, the state-space axes) will yield an approximating parallelepiped; however, the desired property that the approximate degree of controllability be zero if and only if the system is uncontrollable cannot be assured for an arbitrary choice of directions. This becomes evident when we consider a simple example.

In Fig. 1, the rectangle constructed with edges parallel to the state-space axes provides a fairly tight approximation to recovery region 1. However, it yields a much poorer approximation to the degree of controllability ρ_2 of region 2. In fact, if $\rho_2 \to 0$ in such a way that region 2 degenerates to a line forming a diagonal of the rectangle, then the rectangle would yield a nonzero approximate degree of controllability $\bar{\rho}$ for a system which is, by definition, uncontrollable.

To preserve this fundamental characteristic of the degree of controllability, the preceding approach is abandoned in favor of an alternate set of (in general, nonorthogonal) directions. The real eigenvectors and generalized eigenvectors and the real and imaginary parts of the complex eigenvectors and generalized eigenvectors of the A matrix are chosen as the n linearly independent directions in the state space. It has been shown[10] that for these directions the desired property of the approximation can be demonstrated under fairly general assumptions. The choice of a nonorthogonal set of directions leads to a parallelepiped approximation to the recovery region as in Fig. 2.

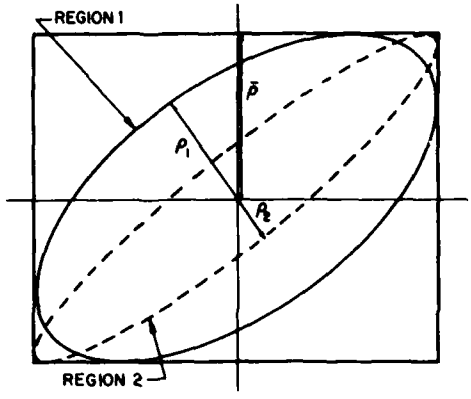

Fig. 1 — Approximation based on the directions of the state-space axes

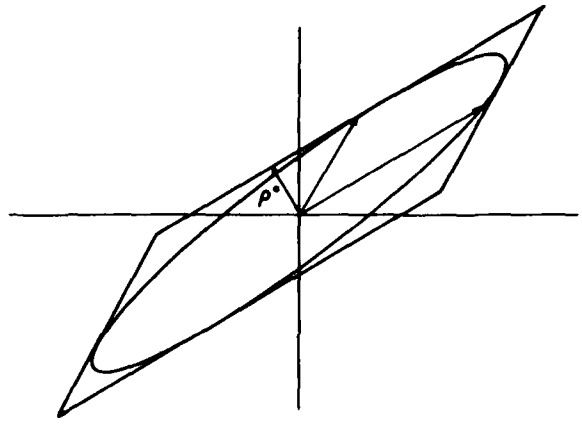

Fig. 2 — Approximation based on a nonorthogonal set of directions

The results of Ref. 8 presented here have been extended in Ref. 10 to handle the special problems which arise in systems with repeated eigenvalues occurring in multiple Jordan blocks. In this case, the essential property, that the approximation be zero if and only if the system is uncontrollable, is maintained through a more sophisticated choice of directions in the state space.

2. APPLICATION OF THE DEGREE OF CONTROLLABILITY TO SIMPLE SYSTEMS

2.1 Introduction

In this section the degree of controllability, as defined in subsection 1.3, is applied to several simple systems for which the exact value of the degree of controllability is readily obtained.

The relation of the degree of controllability to system stability is first investigated. The degree of controllability of three second-order systems—the harmonic oscillator, the damped harmonic oscillator, and the double-integral plant—is then considered. This choice of examples comprises the types of modes occurring in modal representations of typical large flexible space structures. They provide the opportunity to examine several important questions regarding the accuracy of the approximation methods, the possibility of eliminating the specification of the recovery time from the problem by obtaining approximate linear relations, and the impact of normalization of the state on the degree of controllability of the system.

Finally, the results of Ref. 10 motivate an examination of the approximate degree of controllability for systems possessing roots which are nearly identical. Since the approximation technique must be modified when multiple roots exist in independent Jordan blocks, the behavior of the approximation in the limit approaching this situation is considered.

2.2 Relation to Stability

To develop the relationship between the degree of controllability and the stability of a system, we consider the simplest of systems, represented by the scalar first-order differential equation

$$\dot{x}(t) = \alpha x(t) + u, \tag{3}$$

with a bounded control given by

$$|u(t)| \leqslant 1. \tag{4}$$

We wish to evaluate the degree of controllability for $-\infty < \alpha < \infty$ (very stable to very unstable systems) and for various values of recovery time T. Since this is a one-dimensional system, the degree of controllability is simply the maximum magnitude $|x_0|$ of a state which can be returned to the origin in time T.

This is a time-optimal control problem for which the performance index to be minimized is

$$J = \int_0^T L(x,u,t)\, dt = \int_0^T dt \tag{5}$$

and the Hamiltonian to be maximized is

$$H = pf(x,u,t) - L = p\alpha x + pu - 1. \tag{6}$$

Clearly, Eq. (6) is maximized by the control

$$u(t) = \text{sgn}[p(t)].$$

From Hamilton's equations

$$\dot{p} = -\frac{\partial H}{\partial x},$$

we obtain

$$p(t) = C_1 e^{-\alpha t}. \tag{9}$$

Equations (7) and (9) yield

$$u(t) = u = \text{sgn}[C_1], \tag{10}$$

so that the control has a constant value of $+1$ or -1 for all $t > 0$. Solving Eq. (3) for $x(t)$ with $u = \pm 1$, we obtain

$$x(t) = C_2 e^{\alpha t} \mp \frac{1}{\alpha}. \tag{11}$$

From the definition of the degree of controllability, we seek x_0 such that $x(T) = 0$. Applying this boundary condition to solve for C_2, we may write the initial state in terms of the final time as

$$x_0 = \pm \frac{1}{\alpha}(e^{-\alpha T} - 1). \tag{12}$$

Taking the magnitude of x_0 as the degree of controllability ρ, we obtain

$$\rho(\alpha,T) = \left| \frac{1}{\alpha}(e^{-\alpha T} - 1) \right|. \tag{13}$$

Equation (13) is presented graphically in Fig. 3, from which we can make the following general statements:

- For a system with negative real roots ($\alpha < 0$), the degree of controllability as a function of recovery time T is unbounded, and
- For a system with positive real roots ($\alpha > 0$), the degree of controllability is asymptotically limited such that a limiting value of ρ exists as $T \to \infty$.

2.3 Simple Harmonic Oscillator

The system under consideration in this section is a simple harmonic oscillator governed by the second-order differential equation

$$\ddot{y}(t) + \omega^2 y(t) = Ku(t), \tag{14}$$

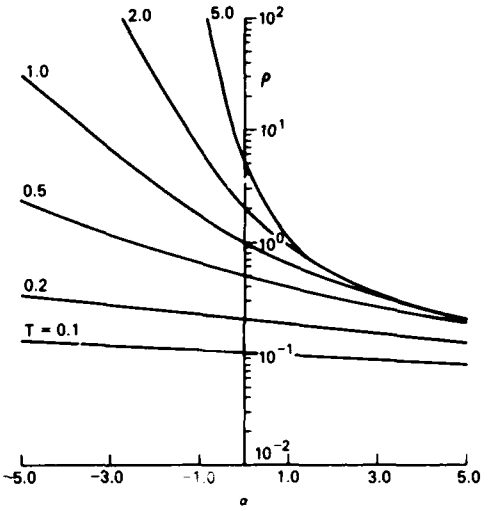

Fig. 3 — Relation between the degree of controllability ρ and stability, as parameterized by α

with the scalar control restricted by

$$|u(t)| \leqslant 1, \quad t > 0. \tag{15}$$

If we choose as state elements

$$x_1 = \frac{\omega}{K}\, y(t), \quad x_2 = \frac{1}{K}\, \dot{y}(t), \tag{16}$$

the system is expressed in first-order form as

$$\begin{bmatrix} \dot{x}_1 \\ \dot{x}_2 \end{bmatrix} = \begin{bmatrix} 0 & \omega \\ -\omega & 0 \end{bmatrix} \begin{bmatrix} x_1 \\ x_2 \end{bmatrix} + \begin{bmatrix} 0 \\ 1 \end{bmatrix} u(t). \tag{17}$$

Equations (16) dictate a particular normalization of the state elements (x_1, x_2). Questions regarding arbitrary normalization of the state are deferred to the discussion of the damped harmonic oscillator in the following section. The motivation for considering the undamped oscillator separately is that the time-optimal-control solution is well known and leads to an expression for the exact degree of controllability in closed form.

The time-optimal control of the system is the familiar bang-bang control of the form

$$u(t) = -\text{sgn}[-\pi_1 \sin \omega t + \pi_2 \cos \omega t], \tag{18}$$

where π_1 and π_2 depend on initial conditions. This control law may be represented graphically be a switching curve in the state space (shown in bold in Fig. 4). The optimal control is then given by

$$u = u(\omega x_1, \omega x_2) = +1, \quad \text{for } (\omega x_1, \omega x_2) \text{ above the switching curve,} \tag{19a}$$

$$u = u(\omega x_1, \omega x_2) = -1, \quad \text{for } (\omega x_1, \omega x_2) \text{ below the switching curve.} \tag{19b}$$

Several resulting characteristics of this solution will aid in the development of the recovery regions associated with the harmonic oscillator:

- The optimal trajectories in the state space lie along concentric circles centered at $(\omega x_1, \omega x_2) = (+1, 0)$ for $u = +1$ and $(\omega x_1, \omega x_2) = (-1, 0)$ for $u = -1$;

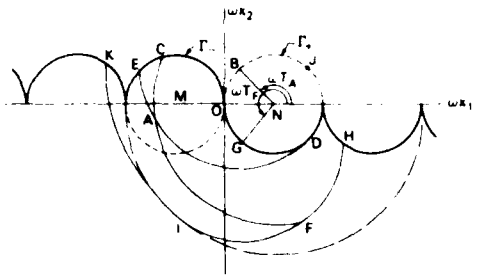

Fig. 4 — Construction of recovery regions for the simple harmonic oscillator

- The relationship between the time of travel along an optimal circular arc and the angle θ defining the arc is given by $\theta = \omega t$ and is independent of the radius of the arc;
- From the control law, Eq. (18), the sign of the control must switch once during the first π/ω time units (provided the state has not reached the origin of the state space);
- The control must change sign every π/ω time units thereafter, until the state is returned to the origin.

Based on these characteristics of the optimal control, the following method of construction for the boundary of the recovery region associated with time T has been developed. (This method is due to Athans and Falb.[12])

In Fig. 4, a typical time-optimal trajectory ACO is shown. Denoting as T_A the time to traverse this trajectory, from the second of the preceding four characteristics we may write

$$\omega T_A = \measuredangle ANC + \measuredangle CMO. \tag{20}$$

To construct the locus of all points in the state space which correspond to the same minimum time to the origin T_A:

1. Construct a circle of radius 2 with center at A, and label the intersection of this circle with the $\Gamma+$ circle as B. (It can be shown by congruent triangles that the angle from the positive ωx_1 axis about N to B is ωT_A.)
2. Construct next a circular arc of radius 2 with center at B connecting the points D and E on $\Gamma+$ and $\Gamma-$ respectively. This defines half of the recovery-region boundary associated with T_A, and the remaining arc may be constructed via symmetry.

Consider now another point F associated with an angle $\omega T_F > \pi$. The optimal trajectory is then FCO. The recovery region is constructed as follows:

1. Begin with a circular arc of radius 2 about F to locate G on $\Gamma+$.
2. The arc HFI of radius 2 is constructed about G.
3. The remainder of the boundary lying below the switching curve is constructed by first locating the point J as the intersection of $\Gamma+$ and an arc of radius 4 about I. (Note that $\measuredangle JNG = \pi$.)
4. An arc of radius 4 centered at J and connecting I and K completes the lower boundary. The upper boundary may again be constructed via symmetry.

The recovery regions for several values of recovery time T are shown in Fig. 5. We note the following properties of the recovery-region boundaries.

- The recovery regions lying wholly within a circle of radius 2 about the origin are bounded by two circular arcs of radius 2 intersecting on the switching curve. The boundary has a cusp at each of these points.
- The recovery regions for $T = i\pi/\omega$, $i = 1, 2, \ldots$, are bounded by circles of radius $2i$ centered at the origin.
- The recovery regions for $T > \pi/\omega$, $T \neq i\pi/\omega$, $i = 2, 3, \ldots$, are bounded by four circular arcs, and the boundary has no cusps. In general, for $j\pi/\omega < T < k\pi/\omega$, the boundary is formed by two arcs of radius $2j$ and two arcs of radius $2k$.
- The centers of all circular arcs which form the above boundaries lie on the $\Gamma+$ or $\Gamma-$ circles. It follows then that for large T the recovery-region boundaries closely approximate circles.

This last result will have important implications when we compare exact and approximate values for the degree of controllability.

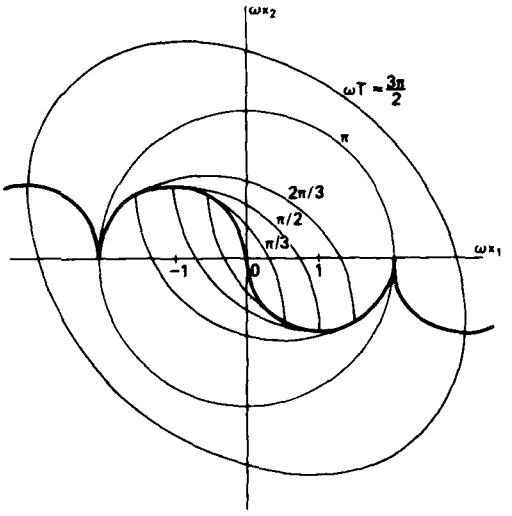

Fig. 5 — Recovery regions for the simple harmonic oscillator

Expressions may now be developed for the minimum distance to the recovery-region boundary associated with a recovery time T. The problem is addressed in two parts, first considering regions wholly contained within the circle of radius 2 and then extending the result to larger regions.

Several constructions are made in Fig. 6. Using the lettering established in Fig. 4 (although with point locations changed somewhat), we note that since the point E lies on the same boundary as A, both points are associated with the same recovery time T_A; therefore $\measuredangle$OME is given by

$$\measuredangle \mathrm{OME} = \omega T_A. \tag{21}$$

By symmetry $\measuredangle$OND = $\measuredangle$OME, and since B, N, and D are collinear (from Fig. 2, N and B are the centers of two arcs which osculate at D), $\measuredangle$ONB is

$$\measuredangle \mathrm{ONB} = \pi - \omega T_A. \tag{22}$$

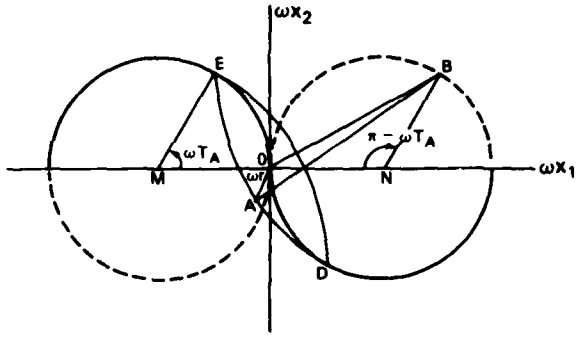

Fig. 6 — Determination of the exact degree of controllability of the simple harmonic oscillator

If A is an arbitrary point on the boundary, the degree of controllability will be determined by minimizing ωr. Since the length OB is fixed for a particular T_A and the length AB is 2, the magnitude of ωr is minimized when B, O, and A are collinear. The length OB is obtained from

$$|OB|^2 = (2 + 2\cos\omega T_A), \tag{23}$$

and then

$$\omega r_{\min} = 2 - \sqrt{2 + 2\cos\omega T_A},\ 0 < \omega T_A < \pi. \tag{24}$$

For $\pi < \omega T < 2\pi$, we recall from Fig. 4 that the boundary arc lying nearest the origin is of radius 4. The minimum distance is therefore given by

$$\omega r_{min} = 4 - \sqrt{2 - 2\cos\omega T},\ \pi < \omega T < 2\pi, \tag{25}$$

and, in general, for $n = 1, 2, \ldots,$

$$\omega\rho(T) = \omega r_{\min} = 2n - \sqrt{2 - 2\cos\omega T},\ (2n-3)\pi \leqslant \omega T \leqslant (2n-2)\pi, \tag{26a}$$

$$= 2n - \sqrt{2 + 2\cos\omega T},\ (2n-2)\pi \leqslant \omega T \leqslant (2n-1)\pi. \tag{26b}$$

Equations (26) constitute an analytic expression for the exact degree of controllability ρ of the simple harmonic oscillator as a function of recovery time T. Attention is now turned toward approximate expressions for the degree of controllability obtained via the methods of Viswanathan, Longman, and Likins.[8]

A parallelogram which superscribes the recovery-region boundary is to be constructed in the state space. The sides of the parallelogram are to be parallel to directions determined by the real and imaginary parts of the eigenvectors of the system matrix. For the system matrix of Eq. (17), the eigenvectors are

$$p_1 = \begin{bmatrix} 1 \\ i \end{bmatrix},\ p_2 = \begin{bmatrix} 1 \\ -i \end{bmatrix}. \tag{27}$$

The parallelogram is therefore a rectangle with sides parallel to the state-space axes, such that each side contains at least one point in common with the recovery region and that no point within the recovery region lies outside the rectangle. The first approximation to the degree of controllability is then defined as the minimum of the set of perpendicular distances to the sides of the rectangle.

For this simple system, this set becomes merely the maximum values of ωx_1 and ωx_2 attained by the points on the boundary associated with recovery time T. It is easily shown (either by the formal procedure presented in Ref. 8 or by examination of Fig. 4) that the distances are given by

$$\omega d_1 = \int_0^T |\sin \omega t|\, dt, \tag{28a}$$

$$\omega d_2 = \int_0^T |\cos \omega t|\, dt. \tag{28b}$$

The approximate degree of controllability is then

$$\omega\rho^* = \min\,[\omega d_1, \omega d_2]. \tag{29}$$

Viswanathan also noted that as a second approximation to Eqs. (28), for T large relative to the period of the oscillator, the integrands in Eqs. (28) may be replaced by $2/\pi$, the average value over a period. This yields an approximation which is linear in time:

$$\omega\rho^{**}(T) = 2T/\pi. \tag{30}$$

A comparison of the exact expression, Eqs. (26), and the approximate expressions, Eqs. (29) and (30), for the degree of controllability of the simple harmonic oscillator is presented in Fig. 7. Both ρ^* and ρ^{**} periodically yield exact values, and for all T greater than twice the period of the oscillator, the exact and approximate values differ by less than 10%. Further insight into the behavior of the approximations is provided upon noting that the values of recovery time for which the approximations are exact correspond to circular recovery regions. The improvement in the accuracy of the approximations for increasing T is therefore a direct consequence of the tendency of the recovery regions to pure circles for large T.

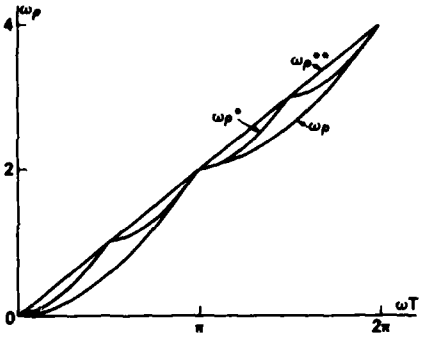

Fig. 7 — Exact values ($\omega\rho$) and approximate values ($\omega\rho^*$ and $\omega\rho^{**}$) of the degree of controllability of the simple harmonic oscillator

2.4 Damped Harmonic Oscillator

The second-order differential equation describing a damped harmonic oscillator may be written

$$\ddot{y}(t) + 2\alpha\dot{y}(t) + (\alpha^2 + \omega^2)y(t) = Ku(t), \tag{31}$$

with the control bounded by

$$|u(t)| \leqslant 1,\ t > 0. \tag{32}$$

Equation (31) can be written in matrix first-order form as

$$\begin{bmatrix} \dot{x}_1' \\ \dot{x}_2' \end{bmatrix} = \begin{bmatrix} -\alpha & \omega \\ -\omega & -\alpha \end{bmatrix} \begin{bmatrix} x_1' \\ x_2' \end{bmatrix} + \begin{bmatrix} 0 \\ 1 \end{bmatrix} u, \tag{33}$$

where

$$x_1'(t) = \frac{\omega}{K} y(t),\quad x_2'(t) = \frac{\alpha}{K} y(t) + \frac{1}{K}\dot{y}(t). \tag{34}$$

At this point, an arbitrary normalization of the state vector may be specified. If weights n_1 and n_2 are chosen for the corresponding elements of x', then Eq. (33) may be written

$$\dot{x} = Ax + Bu, \tag{35}$$

where

$$A = \begin{bmatrix} 1/n_1 & 0 \\ 0 & 1/n_2 \end{bmatrix} \begin{bmatrix} -\alpha & \omega \\ -\omega & -\alpha \end{bmatrix} \begin{bmatrix} n_1 & 0 \\ 0 & n_2 \end{bmatrix} = \begin{bmatrix} -\alpha & n_2\omega/n_1 \\ -n_1\omega/n_2 & -\alpha \end{bmatrix}, \tag{36a}$$

$$B = \begin{bmatrix} 1/n_1 & 0 \\ 0 & 1/n_2 \end{bmatrix} \begin{bmatrix} 0 \\ 1 \end{bmatrix} = \begin{bmatrix} 0 \\ 1/n_2 \end{bmatrix}, \tag{36b}$$

$$x = \begin{bmatrix} 1/n_1 & 0 \\ 0 & 1/n_2 \end{bmatrix} \begin{bmatrix} x_1' \\ x_2' \end{bmatrix} = \begin{bmatrix} x_1'/n_1 \\ x_2'/n_2 \end{bmatrix}. \tag{36c}$$

The time-optimal control solution is obtained via minimization of the Hamiltonian

$$H = -\alpha x_1(t)p_1(t) + \frac{n_2}{n_1}\omega x_2(t)p_1(t) - \frac{n_1}{n_2}\omega x_1(t)p_2(t)$$
$$- \alpha x_2(t)p_2(t) + \frac{1}{n_2}u(t)p_2(t) + 1. \tag{37}$$

(A complete development of the time-optimal control of a damped harmonic oscillator is presented in Ref. 12, pp. 590-595.) The control $u(t)$ which minimizes Eq. (37) is

$$u(t) = -\text{sgn}[p_2(t)], \tag{38}$$

and the costate p_2 is given by

$$p_2(t) = e^{\alpha t}\left(-\pi_1 \frac{n_2}{n_1} \sin \omega t + \pi_2 \cos \omega t\right), \tag{39}$$

where π_1 and π_2 depend on initial conditions. Defining the initial state

$$\xi_1 = x_1(0), \quad \xi_2 = x_2(0) \tag{40}$$

and solving Eq. (35) using the optimal control

$$u = \Delta = \pm 1, \tag{41}$$

we obtain the optimal trajectories (after extensive algebra):

$$\frac{\omega^2 + \alpha^2}{\omega}x_1(t) = \frac{\omega^2 + \alpha^2}{\omega}\xi_1 e^{-\alpha t}\cos \omega t + \frac{n_2}{n_1}\frac{\omega^2 + \alpha^2}{\omega}\xi_2 e^{-\alpha t}\sin \omega t$$
$$- \frac{\Delta}{n_1}\frac{\sqrt{\omega^2 + \alpha^2}}{\omega} e^{-\alpha t}\sin(\omega t + \psi) + \frac{\Delta}{n_1}, \tag{42a}$$

$$\frac{\omega^2 + \alpha^2}{\omega}x_2(t) = -\frac{\omega^2 + \alpha^2}{\omega}\frac{n_1}{n_2}\xi_1 e^{-\alpha t}\sin \omega t + \frac{\omega^2 + \alpha^2}{\omega}\xi_2 e^{-\alpha t}\cos \omega t$$
$$- \frac{\Delta}{n_2}\frac{\sqrt{\omega^2 + \alpha^2}}{\omega} e^{-\alpha t}\cos(\omega t + \psi) + \frac{\Delta\alpha}{n_2\omega}, \tag{42b}$$

where $\psi = \tan^{-1}\frac{\omega}{\alpha}$.

The paths described by Eqs. (42) are logarithmic spirals which tend to the points $\left(\frac{\omega^2 + \alpha^2}{\omega}x_1, \frac{\omega^2 + \alpha^2}{\omega}x_2\right) = \left(\frac{\Delta}{n_1}, \frac{\Delta\alpha}{n_2\omega}\right)$. The equations are transcendental; therefore closed-form

expressions for the trajectories (with time eliminated) cannot be obtained. However, the boundary of the recovery region associated with a specified recovery time T is easily computed numerically using Eqs. (42). Recovery regions for a typical system (with $\alpha = \omega/4$ and $n_1 = n_2 = 1$) are plotted in Fig. 8 along with the switching curve for the system (in bold). The minimum distance ρ to the recovery region as a function of recovery time T may also be obtained numerically.

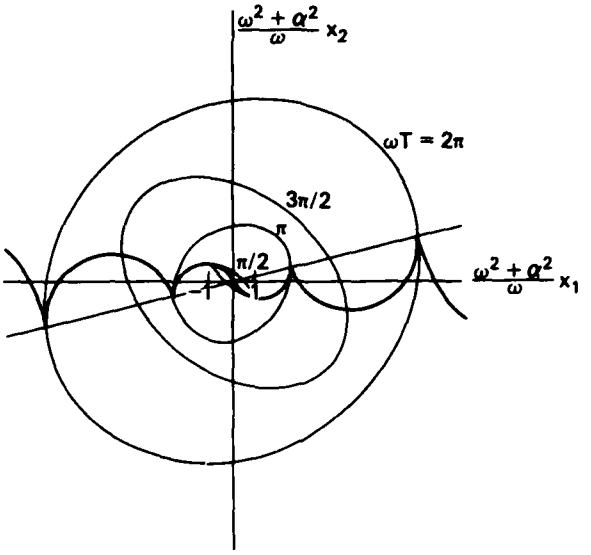

Fig. 8 — Recovery regions for a damped harmonic oscillator with $\alpha = \omega/4$

To obtain the approximate degree of controllability ρ^* for this system, we again consider the eigenvectors of the system matrix. The eigenvectors of A as specified in Eq. (36a) are

$$p_1 = \begin{bmatrix} 1 \\ \frac{n_1}{n_2} i \end{bmatrix}, \quad p_2 = \begin{bmatrix} 1 \\ \frac{-n_1}{n_2} i \end{bmatrix}; \tag{43}$$

hence, as with the undamped oscillator, the directions of interest are the state-space axes. Following the procedure of Ref. 8, we find that the minimum distances to the sides of the superscribed rectangle are

$$d_1 = \frac{1}{n_1} \int_0^T |e^{\alpha t} \sin \omega t| \, dt, \tag{44a}$$

$$d_2 = \frac{1}{n_2} \int_0^T |e^{\alpha t} \cos \omega t| \, dt. \tag{44b}$$

At this point several observations may be made. First, in the case of zero damping ($\alpha = 0$) and unit normalization, Eqs. (44) become identical to Eqs. (28), as expected. In this case the trajectories given by Eqs. (42) become circles centered at $(\omega x_1, \omega x_2) = (\Delta, 0)$, also as expected. We can therefore treat arbitrary normalization of the simple harmonic oscillator as a special case of this problem.

The exact degree of controllability ρ of this system may be compared with the approximate value ρ^*, as defined by

$$\frac{\omega^2 + \alpha^2}{\omega} \rho^* = \min \left[\frac{\omega^2 + \alpha^2}{\omega} d_1, \frac{\omega^2 + \alpha^2}{\omega} d_2 \right]. \tag{45}$$

Figures 9 and 10 make this comparison for two cases, with values of damping α and normalization n_1 and n_2 as noted in the two figure titles.

In the case of unit normalization ($n_1 = n_2 = 1$), Viswanathan, Longman, and Likins again propose a second approximation based on the average value of the integrands of Eqs. (44) over one period. This approximation is given by

$$\rho^{**} = \frac{2}{\pi} \int_0^T e^{\alpha t}\, dt. \tag{46}$$

The values of $\frac{\omega^2 + \alpha^2}{\omega} \rho^{**}$ are also presented, for comparison, in Fig. 9.

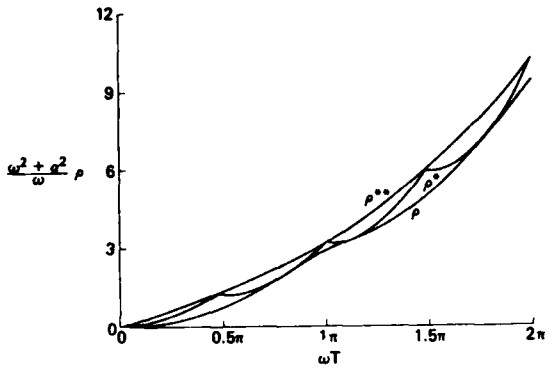

Fig. 9 — Exact values (ρ) and approximate values (ρ^* and ρ^{**}) of the degree of controllability of a damped harmonic oscillator with $\alpha = \omega/4$ and $n_1 = n_2 = 1$

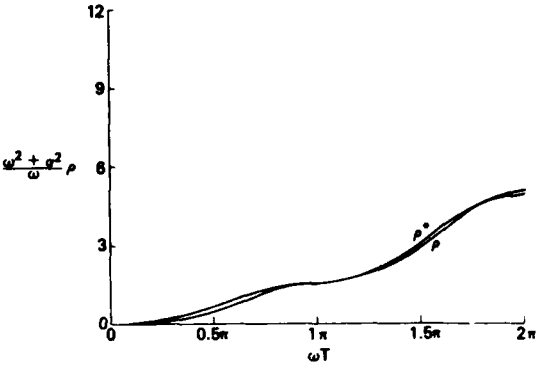

Fig. 10 — Exact values and approximate values of the degree of controllability of a damped harmonic oscillator with $\alpha = \omega/4$ and $n_1 = 2$, $n_2 = 1$

2.5 Double-Integral Plant

To evaluate the relation between exact and approximate values of the degree of controllability of a double-integral plant, the following second-order representation of the system is considered:

$$\ddot{y}(t) = \Gamma u(t), \tag{47}$$

with a bounded control

$$|u(t)| \leqslant 1, \quad t > 0. \tag{48}$$

Written in state-space form, Eq. (47) becomes

$$\begin{bmatrix} \dot{x}_1 \\ \dot{x}_2 \end{bmatrix} = \begin{bmatrix} 0 & \Gamma \\ 0 & 0 \end{bmatrix} \begin{bmatrix} x_1 \\ x_2 \end{bmatrix} + \begin{bmatrix} 0 \\ 1 \end{bmatrix} u, \tag{49}$$

where the state elements have been defined as

$$x_1(t) = y(t), \quad x_2(t) = \dot{y}(t)/\Gamma. \tag{50}$$

The well-known time-optimal regulator control[12] may be written

$$u(t) = -\text{sgn}\left[x_1(t) + \frac{\Gamma}{2} x_2(t)|x_2(t)|\right]. \tag{51}$$

Equivalently, the sign of the bang-bang control defined by Eq. (51) may be determined graphically from a parabolic switching curve in the state space as shown in bold in Fig. 11. The control is positive for states below the switching curve and negative for states above.

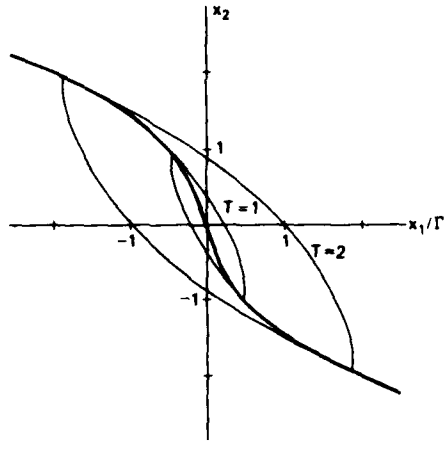

Fig. 11 — Recovery regions for a double-integral plant

The optimal solution is characterized as follows:

- The optimal trajectories in the state space are parabolic and concave to the right for control $u = +1$ and concave to the left for control $u = -1$;
- The control law, Eq. (51), is such that the control will change sign at most once, that being when the trajectory intersects the switching curve;
- The optimal trajectory from that point will follow the switching curve to the origin.

To determine the recovery region associated with a specified recovery time T, we seek the envelope defined by the locus of all states for which the optimal control yields a recovery time of T.

For each point (x_1,x_2) in the state space, there exists a minimum time $t^*(x_1,x_2)$ required to return the state of the system to the origin. That minimum time t^* is the sum of the time required to reach the switching curve and the time required to traverse the switching curve from the point of intersection to the origin.

We consider first those initial states lying on the switching curve. The optimal control is simply

$$u(t) = -\text{sgn}\ (x_2). \tag{52}$$

Integrating the second state equation in this case, we obtain

$$x_2(t) = x_{20} \pm t. \tag{53}$$

From Eq. (53), t^* corresponding to a final state $x_2 = 0$ is then

$$t^*(x_{10},x_{20}) = |x_{20}|, \text{ for } x_{10} = -\frac{\Gamma}{2}\, x_{20}|x_{20}|. \tag{54}$$

For initial states not lying on the switching curve, the control law, Eq. (52), determines the sign of the initial control:

$$u(t_0) = +1, \quad \text{for } x_{10} < -\frac{\Gamma}{2}\, x_{20}|x_{20}|, \tag{55}$$

$$u(t_0) = -1, \quad \text{for } x_{10} > -\frac{\Gamma}{2}\, x_{20}|x_{20}|. \tag{56}$$

We consider first an initial state lying above the switching curve. Using Eq. (56), we integrate the second state equation to obtain

$$x_2 = x_{20} - t. \tag{57}$$

With Eq. (57), integration of the first state equation yields

$$x_1 = x_{10} + \Gamma x_{20} t - \frac{\Gamma}{2} t^2. \tag{58}$$

Denoting as t_a the time required to reach the switching curve, we impose the constraint

$$x_1(t_a) = \frac{\Gamma}{2} x_2^2(t_a). \tag{59}$$

Substituting Eq. (59) into Eq. (58) and solving for t_a, we obtain

$$t_a = x_{20} + \sqrt{\frac{1}{2} x_{20}^2 + \frac{1}{\Gamma} x_{10}}. \tag{60}$$

To determine the remaining time t_b to reach the origin, we note from Eq. (54) that

$$t_b = |x_2(t_a)| = -x_2(t_a), \tag{61}$$

since $x_2(t_a)$ is necessarily negative by the assumption above. Using Eqs. (57) and (60), we rewrite Eq. (61) as

$$t_b = \sqrt{\frac{1}{2} x_{20}^2 + \frac{1}{\Gamma} x_{10}}. \tag{62}$$

Combining Eqs. (60) and (62), we obtain for the optimal recovery time for an arbitrary initial state lying above the switching curve

$$t^* = t_a + t_b = x_{20} + 2\sqrt{\frac{1}{2} x_{20}^2 + \frac{1}{\Gamma} x_{10}}. \tag{63}$$

The procedure may be repeated to obtain an equivalent expression for initial states below the switching curve. Summarizing these results

$$t^*(x_1,x_2) = x_2 + 2\sqrt{\frac{1}{2} x_2^2 + \frac{1}{\Gamma} x_1}, \quad x_1 \geqslant -\frac{\Gamma}{2} x_2|x_2|, \tag{64a}$$

$$= -x_2 + 2\sqrt{\frac{1}{2} x_2^2 - \frac{1}{\Gamma} x_1}, \quad x_1 \leqslant -\frac{\Gamma}{2} x_2|x_2|. \tag{64b}$$

Equations (64) can now be manipulated to obtain expressions for the locus of all states associated with a specified optimal time T:

$$x_1 = -\frac{\Gamma}{4} x_2^2 - \frac{\Gamma}{2} x_2 T + \frac{\Gamma}{4} T^2, \quad x_1 \geqslant -\frac{\Gamma}{2} x_2|x_2|, \tag{65a}$$

$$= \frac{\Gamma}{4} x_2^2 - \frac{\Gamma}{2} x_2 T - \frac{\Gamma}{4} T^2, \quad x_1 \geqslant -\frac{\Gamma}{2} x_2|x_2|. \tag{65b}$$

Typical recovery-region boundaries are shown in Fig. 11.

The exact degree of controllability of the system is obtained by solving for the minimum distance to the boundary defined by Eqs. (65). Since the envelope is symmetric about the origin, it will be sufficient to consider

$$x_1 = -\frac{\Gamma}{4} x_2^2 - \frac{\Gamma}{2} x_2 T + \frac{\Gamma}{4} T^2. \tag{66}$$

The radial distance r may be obtained from

$$r^2 = x_1^2 + x_2^2$$

$$= \frac{\Gamma^2}{16} x^4 + \frac{\Gamma^2 T}{4} x^3 + \left(\frac{\Gamma^2 T^2}{8} + 1\right) x^2 - \frac{\Gamma^2 T^3}{4} x_2 + \frac{\Gamma^2 T^4}{16} \tag{67}$$

Differentiating Eq. (67), we see that the expression for the x_2 component of r_{min} is a cubic in x_2 (from Fig. 9, the extremum is a minimum):

$$\frac{\Gamma^2}{4} x_2^3 + \frac{3\Gamma^2 T}{4} x_2^2 + \left[\frac{\Gamma^2 T^2}{4} + 2\right] x_2 - \frac{\Gamma^2 T^3}{4} = 0. \tag{68}$$

Equation (68) may be solved analytically for $x_{2_{min}}$, and Eq. (66) may then be used to obtain $x_{1_{min}}$. The exact degree of controllability of the system is then given by

$$\rho = \sqrt{x_{1_{min}}^2 + x_{2_{min}}^2}. \tag{69}$$

The approximate degree of controllability for the system is to be determined from the superscribed parallelogram with sides parallel to the directions defined by the real and imaginary parts of the eigenvectors of the system matrix. In this case, since Eq. (49) is in Jordan form, these directions are along the state-space axes. It is easily shown that the distances to the edges of the parallelogram (rectangle) enclosing the recovery region for time T are the magnitudes of the coordinates of the point on the switching curve corresponding to time T. These distances are

$$d_1 = |x_1| = \frac{\Gamma}{2} T^2, \tag{70a}$$

$$d_2 = |x_2| = T, \tag{70b}$$

and the approximation to ρ is

$$\rho^* = \min\left[T, \frac{\Gamma}{2} T^2\right]. \tag{71}$$

The normalization, included earlier in the discussion of the damped harmonic oscillator, has been intentionally omitted from this development. From Eq. (71), the impact of arbitrary normalization of the state elements in this problem can be determined by investigating the behavior of ρ with respect to variation in Γ.

The exact and approximate values for the degree of controllability as a function of recovery time are presented in Fig. 12 for various values of Γ. In each case (and for all values of Γ), the curves diverge, indicating that Eq. (71) yields a progressively poorer upper bound to the actual degree of controllability of the system with increasing recovery time T.

Viswanathan, Longman, and Likins[8] note that the approximation may always be improved by choosing more directions in the state space. However, careful examination of this example will indicate that unless the exact direction of r_{min} is chosen, the resulting approximation will still be divergent.

2.6 Nearly Repeated Roots

Another situation which often occurs in large systems and yet may be studied by simple example is the problem of nearly repeated roots. When a multiple root occurs in more than one Jordan block, a modification of the approximation technique is required to assure that the approximation behaves properly in the limit as the system approaches an uncontrollable configuration. Specifically, Ref. 10 details an alternate choice of directions which should be used in this case for the evaluation of the approximate degree of controllability. (When a multiple root involves only a single Jordan block, the standard set of directions developed in Ref. 8 apply—such is the case with the double-integral-plant problem of the preceding subsection.)

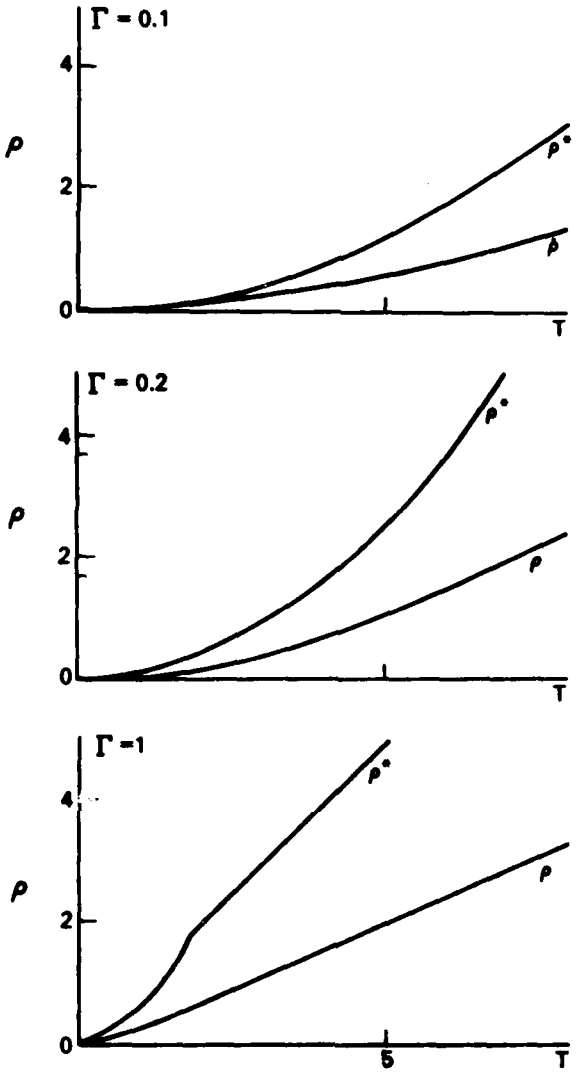

Fig. 12 — Exact and approximate values of the degree of controllability of a double-integral plant

This abrupt change in the approximation technique for this special situation prompts questions regarding the behavior of the approximation in a system which is numerically "near" a multiple-root situation. Such a situation can easily occur as a result of system models which are generated numerically, in that true multiple roots virtually never appear with exactly the same value due to numerical errors involved in developing the model. In what follows, we will clarify what is meant by "near" and will examine two simple two-dimensional problems to gain insight into how such situations should be treated in more complex systems.

Two distinct cases must be considered separately to fully understand the near-multiple-root problem. In each case we will consider the behavior of the degree of controllability in the limit as the system numerically approaches the situation of a repeated root of multiplicity two in two Jordan blocks. In the first case, the limit is approached from a system with a repeated root associated with a single Jordan block; specifically, the problem is

$$\lim_{\epsilon \to 0} A = \lim_{\epsilon \to 0} \begin{bmatrix} \lambda & \epsilon \\ 0 & \lambda \end{bmatrix}. \tag{72}$$

For $\epsilon \neq 0$, the standard choice of directions in the state space outlined in subsection 2.1 applies. However, when $\epsilon = 0$, the modified directions of Ref. 10 must be used to retain the desired characteristic of the approximation. The second way in which the same limit may be approached is when two distinct roots approach the same numerical value. The simplest example of this situation is

$$\lim_{\epsilon \to 0} A = \lim_{\epsilon \to 0} \begin{bmatrix} \lambda & 0 \\ 0 & \lambda + \epsilon \end{bmatrix}. \tag{73}$$

Here again, the standard approximation technique applies except when $\epsilon = 0$. These two problems are fully developed below.

Case I

As always, the system is described by Eqs. (1) and (2), where now

$$A = \begin{bmatrix} \lambda & \epsilon \\ 0 & \lambda \end{bmatrix}, \quad B = \begin{bmatrix} 1 \\ 1 \end{bmatrix}. \tag{74}$$

Here B has been chosen to produce an uncontrollable system in the limit as $\epsilon \to 0$. The left and right eigenvectors of the system matrix A are the columns of the matrices

$$Q = \begin{bmatrix} 1/\epsilon & 0 \\ 0 & 1 \end{bmatrix}, \quad P = \begin{bmatrix} \epsilon & 0 \\ 0 & 1 \end{bmatrix}, \tag{75}$$

and the eigenvector directions (here, the state-space axes) remain distinct as $\epsilon \to 0$. The approximate degree of controllability for this system for time T is obtained by computing the distances to the rectangle, with sides parallel to state-space axes, which superscribes the actual recovery region. Using the procedure presented in Ref. 8, we find these distances to be

$$d_1 = \int_0^T |(1 - \epsilon t)| e^{-\lambda t}\, dt, \tag{76a}$$

$$d_2 = \int_0^T e^{-\lambda t}\, dt. \tag{76b}$$

It is clear from Eqs. (76) that as $\epsilon \to 0$, both of these distances remain nonzero; therefore, the approximate degree of controllability, which is simply $\rho^* = \min [d_1, d_2]$, does not reflect the fact that the system is uncontrollable in the limit. This result is displayed graphically in Fig. 13, which shows the behavior of the recovery region as $\epsilon \to 0$, for $\lambda = 1$ and $T = 1$.

Viswanathan and Longman[10] recognized that the directions defined by the columns of P (or more generally, the real and imaginary components of the columns of P) do not provide a satisfactory approximation when repeated roots occur in multiple Jordan blocks. The system described by Eq. (74) with $\epsilon = 0$ illustrates the difficulty which arises. A more sophisticated choice of directions was subsequently developed which satisfactorily handles this difficulty as a special case of the general problem. The procedure involves replacing a specific subset of the full set of directions with a new modified subset. Here we wish to examine the behavior in the limit as $\epsilon \to 0$ of the approximation obtained by using the procedure developed for the limiting case itself.

Without reiterating the entire general procedure developed in Ref. 10, we summarize its application to this problem by first noting that here the full set of (two) directions will be replaced by a modified set. The modified set is obtained by first performing a singular value decomposition on the matrix $Q^{*T}B$, where Q^* is a matrix containing a specific subset of the columns of Q. For our problem $Q^* = Q$, so we define

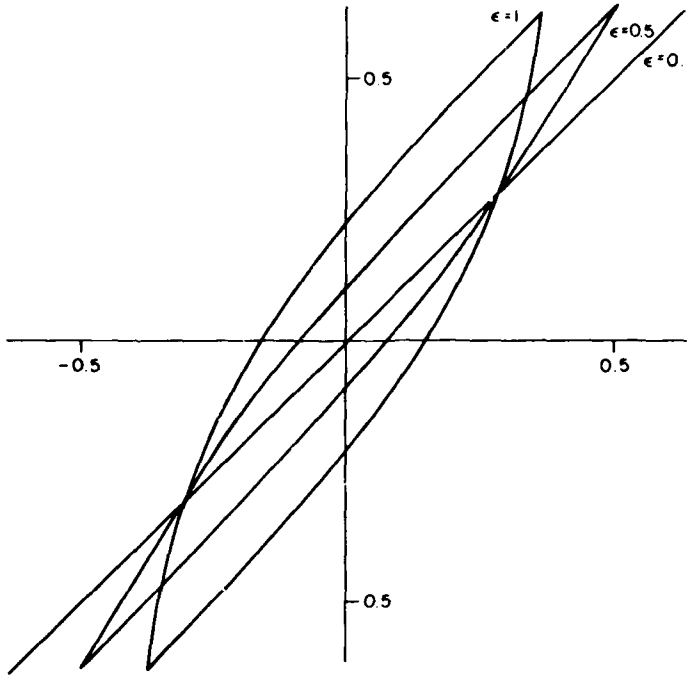

Fig. 13 — Recovery regions as $\epsilon \to 0$ for case I of the problem of nearly repeated roots

$$Q^T B = U \Sigma W. \tag{77}$$

The original directions defined by the columns of the corresponding matrix P^* are replaced with the column directions of P^*U. For this case

$$P^*U = PU = \frac{1}{\epsilon^2 + 1} \begin{bmatrix} \epsilon & \epsilon^2 \\ \epsilon & -1 \end{bmatrix}. \tag{78}$$

We note that these directions are nonorthogonal, leading to an approximating parallelogram with sides parallel to the directions defined by the columns of Eq. (78). The new distances, which now replace those of Eqs. (76), are

$$d_1^* = \int_0^T \frac{2}{3 + \epsilon^4} \, |(1 - \epsilon^2 - \epsilon t)| e^{-\lambda t} \, dt, \tag{79a}$$

$$d_2^* = \int_0^T \frac{1 + \epsilon^4}{1 + 3\epsilon^4} \, |\epsilon t| e^{-\lambda t} \, dt. \tag{79b}$$

We find that the approximation is now properly behaved in the limit in that $\lim_{\epsilon \to 0} d_2^* = 0$. These results may be confirmed by considering again Fig. 13. In the limit, the directions which define the parallelogram are given by vectors $[1\ 1]^T$ and $[0\ 1]^T$. Clearly, for $\epsilon = 0$, the recovery region has degenerated to a line along the direction of $[1\ 1]^T$; thus the distance d_2^* to the side parallel to $[1\ 1]^T$ is zero, as expected.

Case II

The second case to be considered is defined by the matrices

$$A = \begin{bmatrix} \lambda & 0 \\ 0 & \lambda + \epsilon \end{bmatrix}, \quad B = \begin{bmatrix} 1 \\ 1 \end{bmatrix}, \tag{80}$$

where the concern is over the behavior of the approximation when the roots are nearly equal (ϵ small). We note that for the limiting case $\epsilon = 0$, the system is uncontrollable. The left and right eigenvectors are clearly the state-space axes (the system is in Jordan form), and by the standard approximation procedure for nonrepeated roots, the distances to the sides of approximating rectangle are

$$d_1 = \int_0^T e^{-\lambda t}\, dt, \tag{81a}$$

$$d_2 = \int_0^T e^{-(\lambda+\epsilon)t}\, dt. \tag{81b}$$

As $\epsilon \to 0$, we reach the same conclusion as for case I, that the approximate degree of controllability based on Eqs. (81) does not indicate that the system is nearly uncontrollable (since neither d_1 nor d_2 approach zero in the limit).

Following the philosophy developed in case I, we apply the modified approximation technique, developed for the multiple-root situation, to this problem involving nearly multiple roots. Again we find that the set of directions to be replaced is the full set of two original directions defined by the columns of P, hence P^* and Q^* become

$$P^* = P = \begin{bmatrix} 1 & 0 \\ 0 & 1 \end{bmatrix}, \quad Q^* = Q = \begin{bmatrix} 1 & 0 \\ 0 & 1 \end{bmatrix}. \tag{82}$$

As in Eq. (77), a singular value decomposition of $Q^{*T}B$ is performed, and the new directions on which the modified approximation is based are defined by the columns of

$$P^*U = \frac{1}{2}\begin{bmatrix} 1 & 1 \\ 1 & -1 \end{bmatrix}. \tag{83}$$

Since these directions are orthogonal, the new approximation to the recovery region is a rectangle, and the distances to the sides of the rectangle are given by the integrals

$$d_1 = \frac{1}{2}\int_0^T (1 + e^{-\epsilon t})e^{-\lambda t}\, dt, \tag{84a}$$

$$d_2 = \frac{1}{2}\int_0^T (1 - e^{-\epsilon t})e^{-\lambda t}\, dt. \tag{84b}$$

Here again, we find that the modified choice of direction leads to a satisfactorily behaved approximation, since as $\epsilon \to 0$, $d_2 \to 0$, correctly indicating a nearly uncontrollable system.

As a result of considering these two special cases, we may make several recommendations involving the use of degree-of-controllability approximation techniques for systems numerically near a situation of repeated roots in multiple Jordan blocks. The primary conclusion is that it is desirable in such situations to consider both the standard and modified approximation techniques and to take as the final approximation the smaller resulting value (since each approximation is itself an *upper* bound on the degree of controllability).

In the general case, the use of either approximation technique involves the inversion of an $n \times n$ matrix; therefore the recommended procedure involves an extra matrix inversion. Viswanathan, Longman, and Likins[8] showed that any upper-bound approximation may be improved without further matrix inversion by simply choosing additional directions in the state space. The evaluation of the minimum distance to a side perpendicular to such an additional direction is a simple task.

One might be inclined to consider evaluating such distances in the directions indicated by the modified approximation technique, without performing any further matrix inversion. This approach would have worked in case II, since the additional directions to be considered are orthogonal. The reason that this approach will not work in case I (where the new directions are nonorthogonal), and therefore will not work in general, lies in the subtle difference in the way principal and additional directions

are considered. The principal directions (obtained by either the original or modified technique) determine the directions *parallel to which* the sides of the parallelepiped are constructed. The approximating recovery region may be made more accurate by generating additional sides *perpendicular* to new directions in the state space. However it is the use of sides *parallel* to a specific spanning set of directions which assures the desired behavior of the approximate degree of controllability in the limit as the system becomes uncontrollable.

2.7 Summary

The examination of several simple dynamical systems has provided useful insight into the concept of the degree of controllability of a system. It has been shown that a system with bounded controls and unstable poles has an asymptotically limited degree of controllability—in that there is a limiting value of the degree of controllability as the recovery time T approaches infinity. In constrast, the degree of controllability of a system with stable poles may be increased without bound by increasing the recovery time.

For systems with only undamped harmonic modes, a linear approximation to the degree of controllability as a function of time is easily obtained. This approximation is useful, provided the recovery time is larger than twice the period of the lowest-frequency mode of the system. For damped harmonic modes, a linear approximation is not available; however, if there is only light damping (as in a flexible space structure), the linear approximation to the undamped system might be useful. It can be expected, however, that for large values of recovery time the linear approximation will increasingly underestimate the degree of controllability of the system.

The divergence of the approximate degree of controllability associated with the double-integral plant can lead to problems in computing the degree of controllability of dynamical systems in which rigid-body modes are present. If the system is expressed in modal form, this problem could be circumvented by using the exact expression, Eq. (69), for the rigid-body modes of the system; however, if the system cannot be expressed in modal form (for example, if the normalization has been specified relative to some nonmodal formulation of the model), the present approximation method could lead to a significant overestimation of the degree of controllability of the system.

One reasonable solution to this divergence problem is to seek a conservative (lower-bound) approximation to the degree of controllability of general linear time-invariant systems. The development of such an approximation is the subject of the next section.

Finally, we consider the problems which arise in systems which are numerically near a system with repeated roots occurring in multiple Jordan blocks. It is found that an approximate degree of controllability based on a modified set of directions in the state space (originally developed to handle the limiting case itself) provides a satisfactory approximation in a region about the limiting case as well.

3. APPROXIMATION OF THE DEGREE OF CONTROLLABILITY VIA SYSTEM DISCRETIZATION

3.1 Introduction

A new approximation to the degree of controllability is developed here, obtained via discretization of the continuous system. A temporally discretized representation of a given system leads to a new recovery region in the state space which is contained within the recovery region of the original continuous system. The minimum distance to the boundary of this new recovery region provides a *lower* bound to the degree of controllability of the continuous system. This new approach is motivated in part by the divergence of the upper bound in the double-integral-plant problem of subsection 2.5.

The next two subsections formally develop this new approximation and a method for its computation. This is followed by a discussion of examples which illustrate the relation between the new approximation and the original approximation and investigate the behavior of the new approximation with respect to discretization step size.

3.2 Discretization and the Discrete Recovery Region

The proposed approximation to the degree of controllability is obtained via discretization of the continuous system described by Eq. (1). This discretized version of a given system with piecewise-constant controls leads to a recovery region in the state space which is contained within the recovery region of the original continuous system. The minimum distance to the boundary of this new recovery region provides a *lower* bound to the degree of controllability of the continuous system.

The standard approach to discretizing the system described by Eqs. (1) and (2) is developed by first writing the solution of Eq. (1) as

$$x(t) = e^{At}x(0) + e^{At}\int_0^t e^{A\tau}Bu(\tau)\,d\tau. \tag{85}$$

If the total recovery time T is divided into N equal intervals ΔT and the control is restricted to be constant over each interval, then the state at the $(k+1)$th step, in terms of the state at the kth step is

$$x[(k+1)\Delta T] = e^{A\Delta T}x(k\Delta T) + e^{A\Delta T}\int_0^{\Delta T} e^{-A\tau}Bu(k\Delta T)\,d\tau \tag{86}$$

or

$$x_{k+1} = e^{A\Delta T}x_k + \int_0^{\Delta T} e^{-A\lambda}Bu_k\,d\lambda, \tag{87}$$

where

$$x_{k+1} \equiv x[(k+1)\Delta T], \tag{88}$$

$$u_k \equiv u(k\Delta T), \tag{89}$$

$$\lambda \equiv \Delta T - \tau. \tag{90}$$

Defining the time-invariant matrices

$$G(\Delta T) = e^{A\Delta T}, \tag{91}$$

$$H(\Delta T) = \left[\int_0^{\Delta T} e^{-A\lambda}\,d\lambda\right]B, \tag{92}$$

we rewrite Eq. (87) as

$$x_{k+1} = Gx_k + Hu_k. \tag{93}$$

An iterative substitution of Eq. (93) into itself yields an expression for the final state of the system in terms of the initial state $\bar{x}$ and the discrete control sequence:

$$x_N = G^N\bar{x} + \sum_{i=0}^{N-1} G^{N-1-i}Hu_i. \tag{94}$$

Restricting x_N to $x_N = 0$ in Eq. (94) will yield an expression for the set of all initial states $\bar{x} \in \mathcal{R}^n$ which can be returned to the origin in N discrete steps:

$$[G^{N-1}H|G^{N-2}H|\ldots|H]\begin{bmatrix} u_0 \\ u_1 \\ \cdots \\ u_{N-1} \end{bmatrix} = -G^N\bar{x}. \tag{95}$$

This expression may be written more compactly as

$$\bar{x} = -G^{-N}F\mathbf{u}, \tag{96}$$

where

$$F = [G^{N-1}H|G^{N-2}H|\ldots|H], \tag{97}$$

$$G^{-N} = (G^N)^{-1}, \tag{98}$$

$$\mathbf{u} = \begin{bmatrix} u_0 \\ u_1 \\ \cdots \\ u_{N-1} \end{bmatrix} \in \mathcal{R}^{N\times m}. \tag{99}$$

Imposing the control limitation, Eq. (2), on each element of Eq. (99), Eq. (96) may be viewed as a mapping from the $(N \times m)$-dimensional control space (where m is the dimension of the control u_k at each step) to an n-dimensional state space. Here each point in the control space $\mathcal{R}^{N\times m}$ represents an entire control time history, not just an instantaneous value of the control as in the m-dimensional control space of the continuous system. The set of admissible controls dictated by Eq. (2) forms a hypercube centered on the origin of the control space and bounded by orthogonal hyperplanes at unit distance from the origin. The state-space recovery region for the discretized system is the image of this hypercube through the map $-G^{-N}F$. Generically, we must require that $N \times m \geq n$ to assure that the recovery region is not dimensionally deficient. This relationship can be visualized (for $N = 3$, $m = 1$, $n = 2$) in Fig. 14. The boundaries of the actual and approximate recovery regions need not contain points in common, although this is the case in the examples subsequently considered.

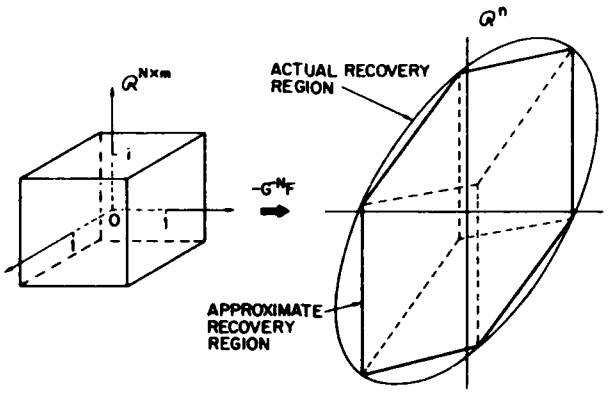

Fig. 14 — Mapping from control space to state space

Several general characteristics of the resulting recovery region may be identified as a result of the convexity of the control hypercube and the linearity of the mapping:

- The recovery region of the discretized system is convex;
- It is bounded by hyperplanes;
- Each hyperplane segment which constitutes a boundary of the recovery region is the image of an $(n-1)$-dimensional boundary segment of the control hypercube.

However, not every $(N-1)$-dimensional boundary segment of the control hypercube maps to a *boundary* segment of the recovery region. In Fig. 14, six edges of the cube form the recovery-region boundary (solid lines), and six edges map to the interior of the recovery region (dashed lines).

3.3 A New Approximation

Based on the preceding development, the following approximation to the degree of controllability is proposed:

Theorem 1. The minimum among the set of perpendicular distances to the hyperplanes of the discretized system recovery region (denoted ρ^*) is a conservative (lower-bound) approximation to the degree of controllability of the continuous system.

The following two propositions establish the validity of the theorem.

Proposition 1. The approximate recovery region R^*, that is, the recovery region of the discretized system, satisfies

$$R^* \subset R. \tag{100}$$

Proof. This result follows directly from the fact that the set of admissible controls for the discrete system is a subset of the set of admissible controls for the continuous system. ■

Proposition 1 establishes the discretized-system recovery region as a conservative approximation to the continuous-system recovery region. The next proposition establishes the proposed approximation as a lower bound to the continuous-system degree of controllability.

Proposition 2. For $N \times m \geqslant n$, ρ^* of theorem 1 satisfies

$$\rho^* \leqslant \rho, \tag{101}$$

where ρ is defined by definition 2 in Subsection 1.3.

Proof. To establish this result, we note first that the perpendicular distance from the origin to an arbitrary boundary hyperplane can be a distance to a point outside R. Such is the case in Fig. 14 for the hyperplanes (lines) which intersect the vertical axis. We will show by contradiction that this cannot occur in the case of the hyperplane that determines ρ^*, which will be sufficient to prove the proposition.

We assume that the minimum among all perpendicular distances, $d_{\min}$, is the distance to a point outside the discrete-system recovery region. There must exist therefore another boundary hyperplane, which we denote j, such that the distance d to that hyperplane along the direction associated with $d_{\min}$ satisfies

$$d < d_{\min}. \tag{102}$$

Since the minimum distance d_j to hyperplane j must satisfy

$$d_j \leqslant d, \tag{103}$$

we have immediately

$$d_j < d_{\min}, \tag{104}$$

which is a contradiction. ■

We consider now the computation of the proposed approximation to the degree of controllability.

Equation (96), the linear transformation from the discrete-system control space to the state space, may be rewritten

$$\bar{x} = K\mathbf{u}, \tag{105}$$

where $K = -G^{-N}F$ and $\mathbf{u}$ is the entire control time history. We wish to determine the state-space recovery-region boundary associated with the set of admissible controls

$$|u_{ik}| \leqslant 1, \; i = 1, 2, \ldots, m, \; k = 1, 2, \ldots, N. \tag{106}$$

As was noted, the boundary of the recovery region, in general, will consist of hyperplane segments associated with $(n-1)$-dimensional boundary segments of the control hypercube given by Eq. (106). However, not every boundary segment of the hypercube will map to a segment of the boundary of the recovery region. In fact, for any given set of parallel $(n-1)$-dimensional boundary segments of the control hypercube, only *two* will map to the boundary of the recovery region. (By virtue of Eq. (106), this pair will be symmetric about the origin.)

These ideas can be clarified by considering once more the specific case of Fig. 14. Here we wish to determine the *one-dimensional* boundary segments of the recovery region; therefore we choose to map the *one-dimensional* edges of the cube through the linear transformation $K = -G^{-N}F$. Under the action of the linear map, parallel lines in the control space are mapped to parallel lines in the state space. In this case, there are three distinct sets of edges, with each set consisting of four parallel line segments. When each set is mapped into the state space, only two lines of each set will be extremal. This result will hold in general, since we always wish to consider segments of dimension one less than that of the state space. The problem of determining an approximate degree of controllability is solved by first finding, for each set of parallel hyperplanes in the state space, the maximum perpendicular distance and then, among these maxima, choosing the minimum as the approximation.

The hyperplanes of a given set are generated by first partitioning the map in Eq. (105) as follows:

$$\bar{x} = [K_1 \; K_2] \begin{bmatrix} \mathbf{u}_1 \\ \mathbf{u}_2 \end{bmatrix}, \tag{107}$$

where $\mathbf{u}_1 \in \mathscr{R}^{n-1}$, $\mathbf{u}_2 \in \mathscr{R}^{(N\times m)-(n-1)}$, and K_1 and K_2 are the corresponding partitions of K.

Each $(n-1)$-dimensional boundary of the hypercube can be characterized by fixing the values of $N \times m-(n-1)$ of the elements of $\mathbf{u}$ and allowing the remaining $n-1$ elements to vary between the limits of $+1$ and -1. Writing Eq. (107) more simply as

$$\bar{x} = K_1\mathbf{u}_1 + K_2\mathbf{u}_2, \tag{108}$$

we note that for K_1 of maximal rank, there exists an n vector $\xi \neq 0$ such that

$$\xi^T K_1 = 0. \tag{109}$$

Multiplying Eq. (27) by ξ^T, we have

$$\xi^T\bar{x} = \xi^T K_2\mathbf{u}_2. \tag{110}$$

Recalling that the elements of $\mathbf{u}_2$ are specified (either ± 1), we recognize Eq. (110) as the equation of a set of hyperplanes in the state space (parameterized by $\mathbf{u}_2$). The perpendicular distance to each hyperplane is given by

$$d = \frac{|\xi^T K_2\mathbf{u}_2|}{(\xi^T\xi)^{1/2}}, \tag{111}$$

where the signs of the elements of $\mathbf{u}_2$ are different for each hyperplane. If we let

$$z^T = \xi^T K_2 \tag{112}$$

and assume

$$|\xi| = 1, \tag{113}$$

then we recognize that the distance to the extremal member of the set of hyperplanes is

$$d_{\max} = \Sigma |z_i|. \tag{114}$$

The computation of the approximate degree of controllability is reduced to determining ξ (typically via Gram-Schmidt orthonormalization) for each possible ordering of the columns in the partition of the matrix K and computing $d_{\max}$ according to Eq. (114). The number of $d_{\max}$ to be computed is equivalent to the number of ways of selecting $n - 1$ columns from the $N \times m$ columns of K. The minimum among the set of all $d_{\max}$ is then the desired approximation.

3.4 Examples

Several considerations motivate the choice of the double-integral plant as our first example. A typical model of a large flexible spacecraft, for which attitude and shape control is desired, will be comprised of both flexible and rigid-body modes, when in modal form. The former take the form of harmonic oscillators, and the latter take the form of double-integral plants. In section 2, we found that while the upper bound developed by Viswanathan provides a tight approximation to the degree of controllability of harmonic systems (and indeed is exact for particular periodic values of T), in the case of the double-integral plant, the approximation diverges from the exact value with increasing recovery time T. This results in a significant overestimation of the degree of controllability. Additionally, this is one of the few simple examples in which the exact degree of controllability can be computed in closed form.

Recalling the work of subsection 2.5, we may write the continuous-system model as

$$\begin{bmatrix} \dot{x}_1 \\ \dot{x}_2 \end{bmatrix} = \begin{bmatrix} 0 & 1 \\ 0 & 0 \end{bmatrix} \begin{bmatrix} x_1 \\ x_2 \end{bmatrix} + \begin{bmatrix} 0 \\ 1 \end{bmatrix} u. \tag{115}$$

In discrete form, the system is represented by Eq. (93) with

$$G = \begin{bmatrix} 1 & \Delta T \\ 0 & 1 \end{bmatrix} \tag{116}$$

and

$$H = \begin{bmatrix} (\Delta T)^2/2 \\ \Delta T \end{bmatrix}, \tag{117}$$

where

$$\Delta T = T/N. \tag{118}$$

We require $N \geqslant 2$ here, since the state space is of dimension two and there is only one control input. Following the new conservative approximation technique of the preceding subsection, we may compute the approximate degree of controllability for various values of discretization number N and recovery time T. Figure 15 presents the new approximation for $N = 2, 4, 8$ along with the exact value and the upper-bound approximation as computed in subsection 2.5.

The accuracy of the approximation is evident from Fig. 16. For $N = 8$, the error is never more than 3%. It is suggested that when N is to be increased to improve the accuracy of the approximation, it should be doubled at each step to assure an improved approximation. This is the logical approach

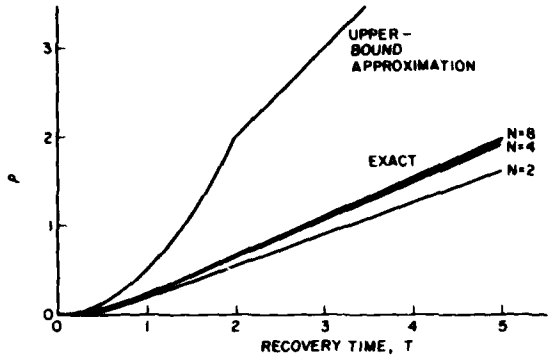

Fig. 15 — Lower-bound approximations (for $N = 2, 4, 8$), exact value, and upper-bound approximation of the degree of controllability for a double-integral plant as a function of recovery time T

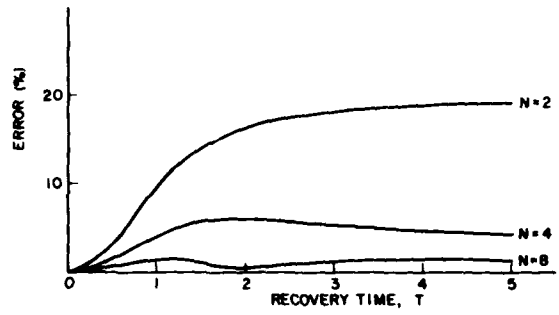

Fig. 16 — Errors for the conservative approximations

when one considers that doubling N results in dividing each discrete control in half. The old set of admissible discrete controls is therefore a subset of the new set of admissible controls, guaranteeing that the approximation converges monotonically to the limit.

The second system considered is a simply supported beam. The model will include the first two modes, with actuators placed at 1/3 and 2/3 the length of the beam.

The continuous system in normalized modal form is represented by the matrices

$$A = \begin{bmatrix} 0 & 2.47 & 0 & 0 \\ -2.47 & 0 & 0 & 0 \\ 0 & 0 & 0 & 9.87 \\ 0 & 0 & -9.87 & 0 \end{bmatrix}, \quad B = \begin{bmatrix} 0 & 0 \\ 0.866 & 0.866 \\ 0 & 0 \\ 0.216 & -0.216 \end{bmatrix}. \tag{119}$$

The value of the approximate degree of controllability for the various values of N and T are illustrated in Fig. 17. For $N = 2$, the approximation is valid over only a very short range of recovery time ($0 < T < 0.25$). Clearly, values of ρ for $T > 0.5$ are meaningless, since the degree of controllability of a linear time-invariant system must increase with increasing recovery time. Curves for $N = 4, 8, 16$ are presented only over the range for which they are monotonically increasing.

It is not surprising that the approximation becomes zero for specific recovery times in the case $N = 2$. A discrete harmonic system is by definition uncontrollable whenever the step size is a multiple of the period of one of the modes. Since N is being held constant, the step size ΔT varies with recovery time T. The periods of the two modes considered here are 2.55 and 0.637. Therefore, when $T = 1.274$ ($\Delta T = 0.637$), the discrete system is uncontrollable; hence the discrete approximation to the degree of controllability is zero.

In light of these results, it is recommended that in determining the approximate degree of controllability over a range of recovery time T, the step size ΔT should be fixed at a value smaller than the period of the fastest oscillator (rather than holding N constant). For a system for which periods are not known, this could be accomplished by first choosing the smallest allowable value of N and increasing the recovery time until the approximation is no longer increasing. Only a value of ΔT within the valid range for that N will lead to satisfactory behavior of the approximation.

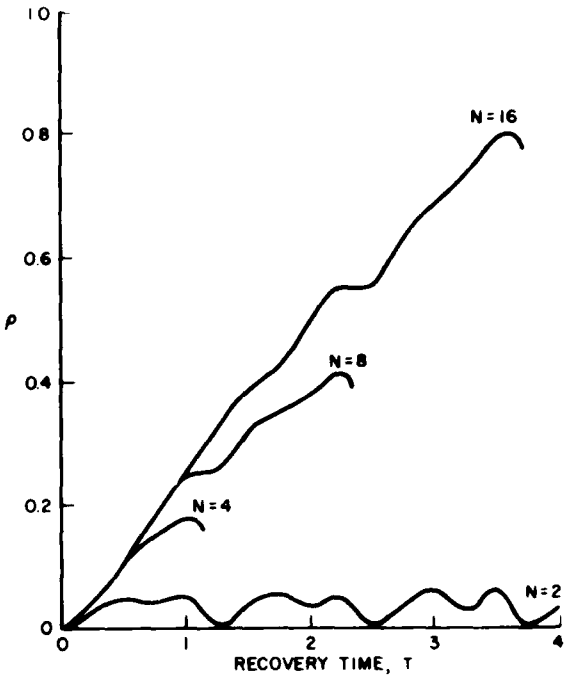

Fig. 17 — Approximate values of the degree of controllability for a simply supported beam

3.5 Summary

A new conservative approximation technique has been developed for estimating the degree of controllability of general linear time-invariant systems. The procedure involves discretization of the continuous system and computation of the degree of controllability of the resulting discrete system. Computation of this value is reduced to performing a Gram-Schmidt orthonormalization on the columns of a linear mapping from the discrete control space to the state space.

The new approximation is shown to avoid the divergence problem associated with the original approximation technique. Discussion of a simple example leads to a straightforward approach to selecting the appropriate step size for the discretization.

4. ACTUATOR PLACEMENT USING DEGREE-OF-CONTROLLABILITY CRITERIA

4.1 Introduction

The placement of actuators for the control of distributed-parameter systems remains an important open question which has received much attention in the last several years. The approaches to resolving the problem are nearly as numerous as the investigators who have addressed it.

Juang and Rodriguez[13] propose to choose locations to minimize a quadratic performance functional based on the steady-state solution of the optimal control and estimation problem. They treat, by example, the placement of a single actuator. Aidarous, Gevers, and Installé[14] obtain optimal actuator-placement solutions by optimizing locations after obtaining an optimal feedback-control-law structure which functionally depends on the actuator locations. The technique is applied to parabolic distributed-parameter systems. Martin[15] considers the problem of optimizing actuators at each point in time and arrives at a dynamic actuator-allocation strategy. Hughes and Skelton[16] examine the controllability (observability) of each mode of the structure as a function of the location of a single actuator (sensor) and suggest that the technique may be employed to optimize multiple actuator (sensor) locations.

Wang and Pilkey[17] use a criterion reflecting the desire to maximize the damping ratio of a particular mode and imply an extension of the technique to a system of modes. The optimization is achieved via classical root-locus techniques. Baruh and Meirovitch[18] find that by use of a design technique known as Independent Modal Space Control (IMSC), the actuator locations have no influence on the feedback control law. They suggest that actuator locations are therefore unimportant when IMSC is used. This has raised some serious questions which will be addressed in detail in section 6.

Skelton and Chiu[19] suggest treating the problem in a unique fashion by first specifying a discrete finite set of possible actuator locations. Initially an actuator is assumed to be at each possible location, the contribution of each to the total system performance is evaluated, and those contributing the least are then eliminated. The optimality of such an approach has yet to be determined.

Kissel and Lin[20] place paramount importance on eliminating all interaction between the control system and a set of known residual modes which have been truncated from the control system model. The design approach couples the actuator-placement and control-law design steps. It is found that a large number of actuator commands must be constrained to achieve the desired isolation, and a small number of actuators are subsequently available for realizing the desired control objective. Schulz and Heimbold[21] also integrate the design steps for actuator (and sensor) location and control-law generation and optimize the design to maximize the dissipation energy due to the control action.

The contribution of the previous two sections to the concept of a degree of controllability (as defined by Viswanathan, Longman, and Likins[8]) are also motivated by the problem of actuator placement. Viswanathan's degree of controllability is clearly not the only such definition possible; indeed several others have subsequently been developed, motivated by this early work. Laskin, Longman, and Likins[22] base a definition of the degree of controllability on a recovery region which reflects both the time and fuel available to accomplish the control objective. In effect, an infinite set of degree-of-controllability criteria result, parameterized by the ratio of fuel available to time available. In the limit as the fuel available becomes infinite, the criterion approaches Viswanathan's definition, and in the limit as time available becomes infinite, the definition yields a fuel-optimal degree of controllability. Paralleling these results, Longman and Alfriend[23] define an energy-optimal degree of controllability which may be associated with the control objective which minimizes control effort. This development is along the lines of Moore[24] and serves to formalize similar work by Arbel and Gupta[25] and Arbel[26] into a consistent framework with other forms of the degree of controllability. In a slight modification of these ideas, Vander Velde and Carignan[27] consider a weighted expression based on the volume of the energy-optimal recovery region and include the possibility of actuator failure in the placement of actuators.

In the next subsection, we will focus on the time-optimal, fuel-optimal, and energy-optimal degree-of-controllability definitions of Refs. 8, 22, and 23 respectively. Upon establishing the definitions of the fuel and energy criteria, we will summarize methods of approximation which are suitable for modal systems. In the subsequent subsection, we will apply these criteria to optimization of actuator locations for control of transverse vibration of a simply supported beam. Although this particular dynamical system is certainly not representative of flexible spacecraft, there are several reasons for considering it. The resulting actuator-placement solutions are easily interpreted, since the mode shapes which describe transverse vibration of the simply supported beam are sine functions. Also, in contrast with the free-free beam problem, the resulting optimal actuator-placement solutions are nontrivial. (This will be discussed in more detail in section 5.) Finally, the difficulties encountered in finding the global optimum for such a simple problem reflects the enormous complexity expected in treating a realistic spacecraft design.

4.2 Alternative Definitions of the Degree of Controllability

The first of the three forms of the degree of controllability to be used here as an actuator-placement criterion is that of Ref. 8, as established by definitions 1 and 2 in subsection 1.3. To distinguish this form from the others to be defined, we will here refer to ρ as the *time-optimal* degree of controllability and use the notation ${}_t\rho$. This reflects the fact that the assumption of a time-optimal control is implicit in definition 2. Similarly, the recovery region established by definition 1 is now denoted ${}_tR$.

By augmenting the system described by Eqs. (1) and (2) with a constraint on the quantity of fuel available, the following definitions may be made[22]:

Definition 3. The *recovery region for time* T *and fuel* F for the normalized system described by Eqs. (1) and (2) is the set

$$ {}_{tf}R = \{x(0) \mid \exists\, u(t),\ t \in [0,T],\ |u_i(t)| \leqslant 1,\ i = 1, 2, \ldots, m, \sum_{i=1}^{m} \int_0^T |u_i(t)|\, dt \leqslant F,\ \ni x(T) = 0\}. $$

Definition 4. The *degree of controllability in time* T *and fuel* F *of the solution* $x = 0$ of the normalized system described by Eqs. (1) and (2) is

$$ {}_{tf}\rho = \inf ||x(0)|| \ \forall\ x(0) \notin {}_{tf}R. $$

This definition of a degree of controllability is parameterized by the ratio of time available to fuel available, and it is interesting to consider the implications of the definition in the limits. As the fuel available becomes large, it reaches a point at which it ceases to have any influence on the control solution. Specifically, if $F \geqslant mT$, the time available is the only constraint on the control solution, since mT is the maximum fuel which can be consumed in time T by m bounded actuators satisfying Eq. (2). In this case ${}_{tf}\rho \equiv {}_t\rho$. In the contrasting limit, as T approaches infinity, the time constraint ceases to influence the control solution, and definitions 3 and 4 lead to what is known as the fuel-optimal degree of controllability Following our new notation convention, we define ${}_f\rho = \lim_{T\to\infty} {}_{tf}\rho$.

The energy-optimal degree of controllability[23] derives from the optimal-control policy which minimizes the performance functional

$$ J(u,T) = \frac{1}{2} \int_0^T u^T u\, dt. \tag{120} $$

Since Eq. (120) limits the control effort, the constraint imposed by Eq. (2) in the earlier definitions is now lifted. (The assumption remains that the control is normalized such that equal magnitudes of the u_i are equally important.) With this, we make the following formal definitions:

Definition 5. The *recovery region for time* T *and energy* E for the normalized system described by Eq. (1) is the set

$$ {}_eR = \{x(0) \mid \exists\, u(t),\ t \in [0,T],\ J(u,T) \leqslant E,\ \ni x(T) = 0\}. $$

Definition 6. The degree of controllability for time T *and energy* E *of the solution* $x = 0$ for the normalized system described by Eq. (1) is defined as

$$ {}_e\rho = \inf ||x(0)|| \ \forall\ x(0) \notin {}_eR. $$

Upon defining ${}_t\rho$, ${}_f\rho$, and ${}_e\rho$, Refs. 8, 22, and 23 respectively address the task of computing the controllability measures. In the time-optimal and fuel-optimal cases, approximate methods are required, since the exact value is not in general obtainable in closed form. For the energy-optimal

criterion, it is easily shown that the exact value is a simple function of the minimum eigenvalue of the controllability Gramian.

In the special case of systems that are described (as spacecraft often are) by undamped modal equations of the form

$$\ddot{\eta}_i + \omega_i^2 \eta_i = \Gamma_i^T u, \quad i = 1, 2, \ldots, n, \tag{121}$$

there exist elegant approximate expressions for all three criteria under consideration. The linear approximation to the time-optimal degree of controllability for an oscillatory system has already been considered in subsection 2.3. Similar approximations are developed in detail in Refs. 22 and 23. In consistent notation, these approximations are

$$_t\bar{\rho} = \frac{2T}{\pi} \min_i \frac{||\Gamma_i||_1}{\omega_i N_i}, \tag{122}$$

$$_e\bar{\rho} = \sqrt{ET} \min_i \frac{||\Gamma_i||_2}{\omega_i N_i}, \tag{123}$$

$$_f\bar{\rho} = F \min_i \frac{||\Gamma_i||_\infty}{\omega_i N_i}. \tag{124}$$

Here N_i in each case is the weighting factor applied to mode i. These three simple approximations, based on norms of the rows of the input influence matrix, will be used in the next subsection to optimize actuators on a simply supported beam.

4.3 Optimal Actuator Placement for a Simply Supported Beam

To gain insight into the behavior of the various optimization criteria summarized in the previous section, we consider here the optimal placement of m force actuators on a simply supported beam, modeled by its n lowest frequency modes. The well-known expression (found in, for example, Ref. 28) for the mode shapes and frequencies of transverse oscillation of a simply supported beam may be written

$$\phi_i(x) = \sin \frac{i\pi x}{L}, \tag{125}$$

$$\omega_i = (i\pi)^2 \sqrt{EI/mL^4}. \tag{126}$$

For our purposes it will suffice to assume the beam to be of unit length ($L = 1$) and the remaining constants (E, I, and m) to be arbitrary. The important property of the frequency expression, Eq. (126), will be found to be the ratio of frequencies, that is,

$$\omega_i/\omega_j = (i/j)^2. \tag{127}$$

For this simple problem, the input influence coefficient Γ_{ik} of the kth actuator on the ith mode is

$$\Gamma_{ik} = \phi_i(p_k) = \sin i\pi p_k. \tag{128}$$

The simplest version of this optimization problem is to place one actuator based on a model which includes only the fundamental mode of the system ($m = 1$, $n = 1$). The obvious optimal solution using any of the three criteria, Eqs. (122), (123), and (124), is to place the actuator at $p_1 = 0.5$, that is, at the middle of the beam, which is the point of maximum deflection of the first mode. Adding mode 2 to the system model produces the simplest problem for which the modal weights N_i influence the optimal solution. Figure 18 illustrates the optimal actuator location as a function of N_1 with $N_2 = 1$ held constant.

For $N_1 < 2.828$, we find that the importance of mode 2 is sufficient to dictate that the actuator be placed at $p_1 = 0.25$, the point of greatest deflection of the second mode. (The first mode *is* controllable from this location.) As we place prime importance on mode 1 by increasing N_1, we see that the

optimal actuator location asymptotically approaches $p_1 = 0.5$. Since mode 2 has a node at 0.5, the actuator cannot be placed exactly at that point unless $N_2 = 0$. The dashed line at $N_1 = 4$ reflects what may be considered a balanced weighting of the modes, that is $N_1/N_2 = \omega_2/\omega_1$. For these weights $p_1 = 0.333$. In general, choosing weights $n_i = 1/\omega_i$ reflects the expectation that, on the average, the energy will be equally distributed among the modes.

As may be expected, the locus of optimal actuator locations displayed in Fig. 18 tells only half the story. The symmetry of the physical system demands that a mirror image of this locus lie in the range 0.5 to 0.75. A simple gradient search procedure will converge to points on this equally optimal locus when the initial actuator location for the search lies in the range 0.5 to 1.0.

It is not surprising that controlling the first two modes with two actuators leads to optimal actuator locations which are symmetric about the center of the beam, each at a location which is optimal for a single actuator (Fig. 19). Although not reflected in the figure, the nature of the solutions is such that with, for instance, $N_1 = 4$, $N_2 = 1$ it is equally desirable to colocate actuators at 0.333 as to place them at (0.333, 0.667). In such a situation, it is left to engineering judgment to determine which of these optimal solutions is more acceptable in the light of other physical considerations. In the sequel, we always present the solution which maintains one actuator on each side of the midpoint of the beam. In every case, moving an optimally located actuator to its mirror location with respect to the midpoint will not change the degree of controllability of the system.

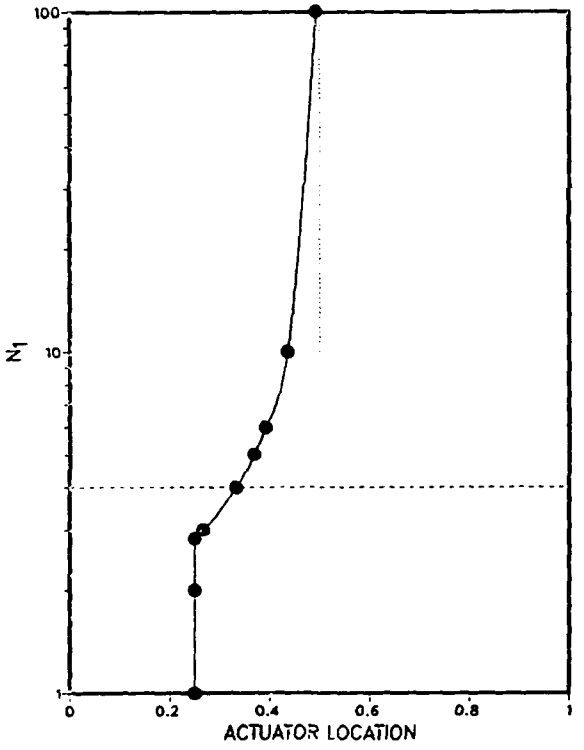

Fig. 18 — Optimal placement of one actuator when a two-mode model is assumed, with $N_2 = 1$. These results apply to the time-optimal, energy-optimal, or fuel-optimal criterion.

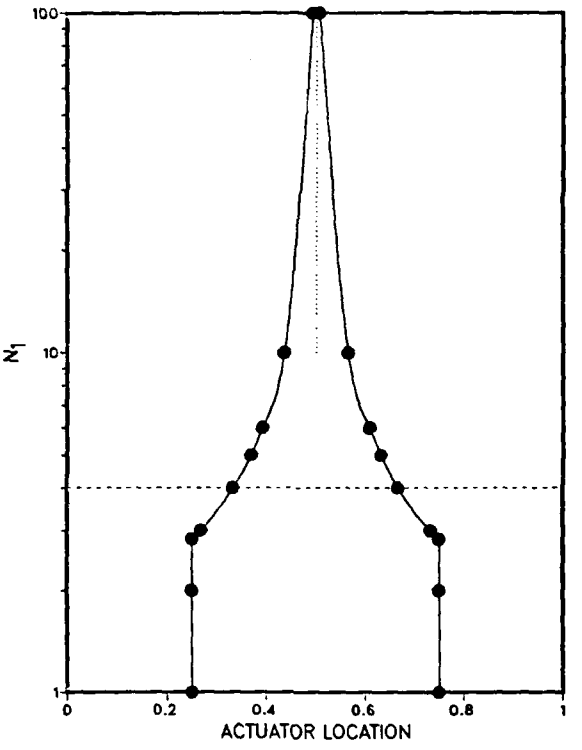

Fig. 19 — Optimal placement of two actuators when two modes are assumed, with $N_2 = 1$. These results apply to the time-optimal or energy-optimal criterion.

The optimal actuator locations shown in Fig. 18 are independent of the particular form of the degree-of-controllability criterion used. The results presented in Fig. 19 hold for both the time-optimal and energy-optimal criteria. (We will discuss the results for the fuel-optimal criterion for this case later.) In general, results using different criteria will be identical either in the case of placement of a single actuator (since the rows Γ_i of the input influence matrix each contain only one element, for which all norms are equal) or whenever two criteria each produce optimal placement of a pair of actuators which are symmetric about the midpoint (since the beam is then equally controllable from either actuator, which implies that there is no better location for a single actuator, so that the case of single-actuator placement holds implicitly).

The preceding discussion may lead one to ask: is there any problem for which the optimal placement of a pair of actuators on a symmetric structure leads to a nonsymmetric solution? We need only add one more mode to the model to encounter just such a situation.

The optimal placement of two actuators assuming a three-mode model of a simply supported beam is considered in Figs. 20 through 23. Figures 20, 21, and 22 display the results using the time-optimal degree of controllability. If N_1^0, N_2^0, N_3^0 are defined as the balanced weights which satisfy $N_i/N_j = \omega_j/\omega_i$, the three figures reflect the variation of N_1, N_2, and N_3 respectively, while the remaining weights are held constant. In each case, the solutions include ranges for which the actuator pair has symmetric locations and ranges for which the locations may be described as complementary.

Focusing our attention on Fig. 20, we may examine these results in more detail. When mode 1 is considered relatively unimportant ($N_1/N_1^0 < 0.6$), the solution set (0.2,0.8) optimally provides a balanced controllability between modes 2 and 3. As the importance of mode 1 increases, the optimal locations move toward the center of the beam, providing greater control authority over mode 1 at the expense of the remaining two. Near the ratio $N_1/N_1^0 = 0.9$, there is a discontinuity in the optimal solution, and a complementary pair of actuator locations (0.2,0.6) is found to be optimal. (By earlier arguments, the sets (0.2,0.4), (0.4,0.8), and (0.6,0.8) are equally optimal in this case.)

This pair of locations is termed complementary, since although neither actuator is placed at the optimal location for a single actuator, they complement each other in providing control authority over the entire system. The actuator at 0.2 provides good balanced control of modes 2 and 3 at the expense of mode 1, and the actuator at 0.6 provides better control authority of mode 1 than either mode 2 or 3. (The optimal location of a single actuator for the same system is shown as a series of open circles over the range for which complementary solutions are optimal.)

The dotted lines extending in either direction from the discontinuity reflect the existence of suboptimal solution sets past the point of discontinuity. In fact the set (0.25,0.75) is a suboptimal (locally optimal) solution for the balanced weighting condition denoted by the horizontal dashed line. Such suboptimal solutions often exist at points of discontinuity. The dotted lines are omitted in Figs. 21, 22, and 23 for clarity.

As the importance of mode 1 is further increased, we see a return to a symmetric pair of locations which again asymptotically approach the center of the beam. Similar results, involving both symmetric and complementary sets of solutions, occur when N_2 and N_3 are varied with respect to their nominal values (Figs. 21 and 22).

Figures 20, 21, and 22 apply only to the time-optimal criterion. As was noted, when two criteria each indicate a symmetric pair of locations for this problem, the solutions are necessarily identical. When complementary solutions are found to be optimal, however, the optimal solutions can, and do, differ. A comparison of the optimal solutions for a variation of N_1 using the time-optimal and energy-optimal criteria is shown in Fig. 23 over the range for which solutions are complementary.

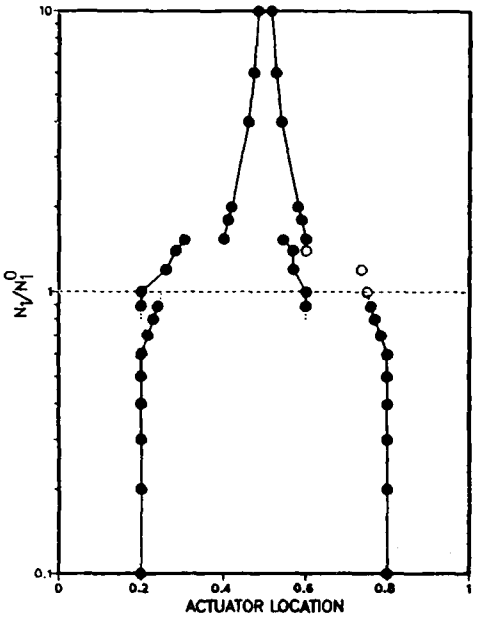

Fig. 20 — Optimal placement of two actuators when three modes are assumed, with N_2 and N_3 held constant. (The open circles indicate the equivalent optimal locations of a single actuator.) These results apply to the time-optimal criterion.

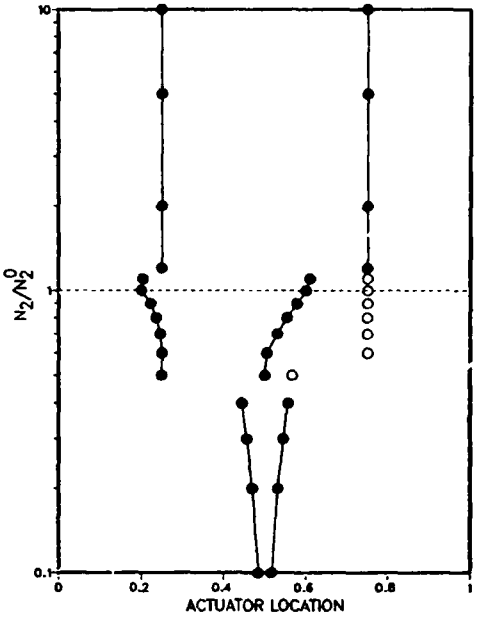

Fig. 21 — Optimal placement of two actuators when three modes are assumed, with N_1 and N_3 held constant. These results apply to the time-optimal criterion.

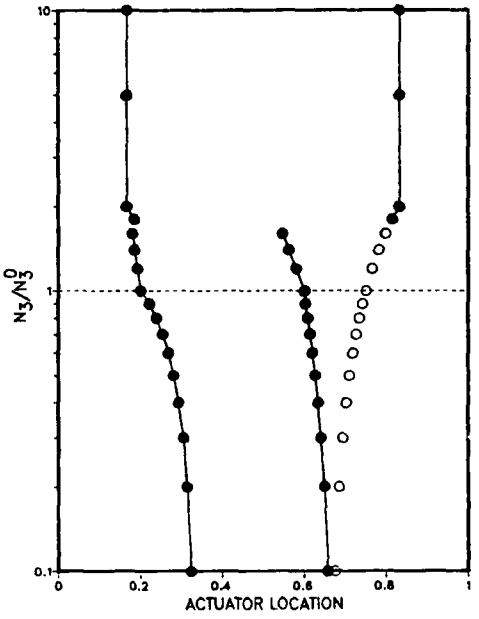

Fig. 22 — Optimal placement of two actuators when three modes are assumed, with N_1 and N_2 held constant. These results apply to the time-optimal criterion.

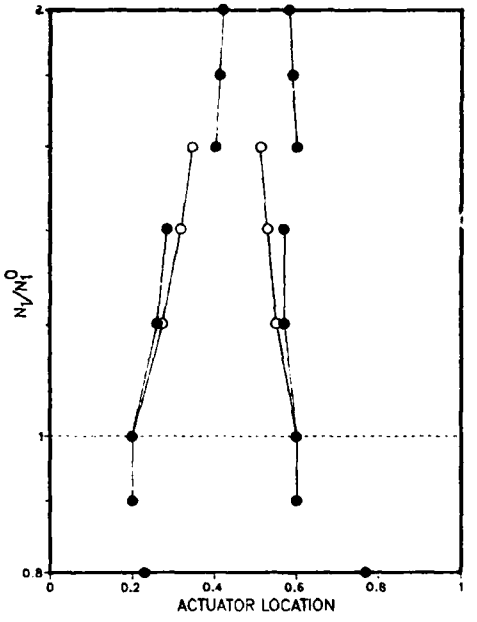

Fig. 23 — Optimal placement of two actuators when three modes are assumed, with N_2 and N_3 held constant. The filled circles apply to the time-optimal criterion, and the open circles apply to the energy-optimal criterion.

The use of the fuel-optimal degree of controllability for multiple-actuator problems yields strikingly different results. Figure 24 summarizes the optimal placement of two actuators when a two-mode model of the beam is assumed. This figure may be compared with Fig. 19, which reflects the results using either the time-optimal or the energy-optimal criterion for the same problem. We find an indeterminancy in the optimal solution for all but one value of N_1 considered. When the first mode is less important, one actuator is optimally placed at 0.25, while a continuum of equally favorable positions exists for the second actuator. If mode 1 is considered more important than mode 2, one actuator is placed at 0.5, and again the second actuator may occupy any location within a specified range. This indeterminancy manifests itself as a result of the nature of the norm in the optimization criterion, Eq. (124). Since the criterion considers only the maximal element of each row Γ_i, often one or more of the actuators have no influence on the optimal solution. This property was first discussed by Laskin.[29] One interesting consequence is that for this particular problem, the set (0.25,0.5) is optimal irrespective of the modal weights. In Fig. 24 we have again limited each of the actuators to half of the beam simply to facilitate the graphical display. Indeed for $N_1/N_1^0 \leqslant 0.7$, the second actuator is free to be placed *anywhere* on the beam (including the endpoints), since it has *no* influence on the optimization criterion.

The results using the fuel-optimal criterion for the three-mode, two-actuator problem and varying N_1 may be summarized as follows. For $N_1/N_1^0 \leqslant 0.7$, the first actuator is optimally placed at either 0.25 or 0.75, and the second actuator is optimally placed at 0.167, 0.5, or 0.833. For the range $0.8 \leqslant N_1/N_1^0 \leqslant 1.0$, the first actuator still is placed either at 0.25 or 0.75, but the second actuator must be placed at 0.5. For $N_1/N_1^0 > 1.0$, the optimal locations are identical to those of Fig. 24. These results may be compared with those of Figs. 20 and 23, which summarize the time-optimal and energy-optimal solutions for the same problem.

We could spend an inordinate amount of time examining this simple example of actuator placement. It will suffice, for the purpose of this work, to consider one further variation on the problem. In Fig. 25, the optimal placement of two actuators is shown as a function of model fidelity, that is, the number of modes considered. In each case the modal weights satisfy $N_i/N_j = \omega_j/\omega_i$. We find that when three or more modes are included, a complementary (rather than symmetric) set of actuator locations appears to be optimal in all cases. This result is reasonable in hindsight but was not the anticipated solution.

It is difficult to make many general statements about this last set of results except to point out that due to the complexity of even this simple problem and behavior of the simple gradient search procedure used, the global optimality of these results is not assured for $n > 4$. (The difficulty of the problem is evidenced by the discrepancy between these results and those of Laskin,[29] who considered the same problem but employed a different search algorithm.)

5. DEGREE OF CONTROL SPILLOVER

5.1 Introduction

Near the end of subsection 4.1, we alluded to a single trivial result which arises when the various degree-of-controllability criteria are applied to the actuator-placement problem for a free-free structure (the simplest of which is the free-free beam). With the insight gained from considering the simply supported beam of section 4, we can now elucidate that statement.

The three optimization criteria, Eqs. (122), (123), and (124), tend to place force actuators at points of maximum deflection of the modes whenever possible and otherwise to find points for which the deflections of the various modes are balanced with respect to the assigned modal weights. For free-free structures, the points of maximum deflection of *all* modes occur at the perimeter of the structure (the ends of a beam, the edges of a plate, etc.). The optimal location of any number of actuators is always at the perimeter of the structure, irrespective of the number of modes in the model or the modal weights assigned.

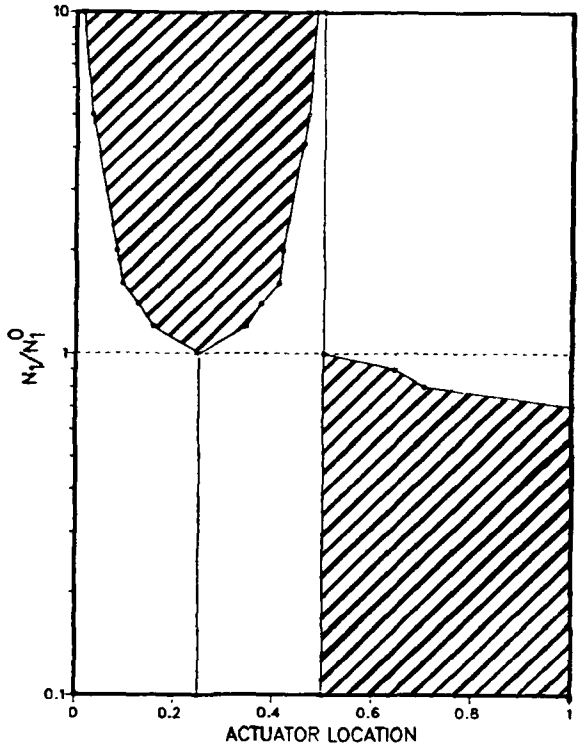

Fig. 24 — Optimal placement of two actuators when a two-mode model is assumed, with $N_2/N_2^0 = 1$. These results apply to the fuel-optimal criterion.

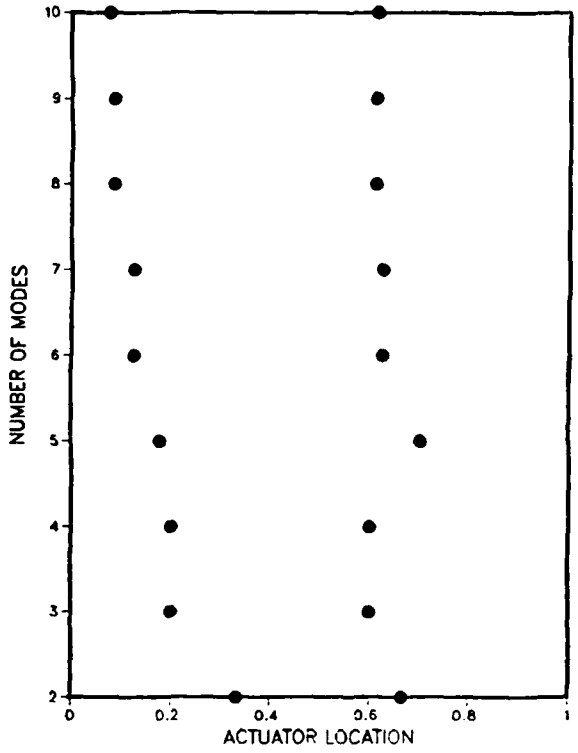

Fig. 25 — Optimal placement of two actuators as a function of the number of modes modeled when the time-optimal criterion is used

Others have reported[8, 16, 27] encountering this problem and have found it to be unsatisfactory from an engineering standpoint. The result can be circumvented by mandating that actuators not be co-located and then limiting the possible actuator locations to a discrete set of points along the structure. This does not, however, obviate the fact that the model is maximally controllable, in terms of the degree of controllability, when all the actuators are placed at the ends of the structure.

The key to this last statement is the word *model.* Although all engineering design is predicated on the assumption that the mathematical model on which a design is based is a reasonable representation of the physical system, it often becomes necessary in practice to accommodate the errors in that same model. In our problem the errors are manifested primarily in the assumption that many modes of the system exist which have not been included in the design of the control system.

Placing all actuators at the ends of a free-free structure is intuitively unsatisfactory in part because we recognize that, as well as providing the greatest control authority over the modeled modes, the end-points provide the greatest opportunity for exciting the unmodeled or residual modes of the system. To account for the effect of the control on the residual modes of the system, it is necessary to quantify the influence of the actuator locations on residual modes of the system and to augment the degree of controllability to account for the existence of control spillover. (Control spillover is a descriptive term coined by Balas[30] which refers to the effect of a control on unmodeled system modes.)

5.2 A Definition for the Degree of Control Spillover

Consider a set of residual modes not included in the control-system model, described by the linear vector-matrix differential equation

$$\dot{x}_r(t) = A_r x_r(t) + B_r u(t). \tag{129}$$

Here, $x_r \in \mathscr{R}^r$, and we assume the residual state vector has been normalized such that unit magnitudes of the elements of $x_r(t)$ are held to be of equal importance. We restrict this development to the time-optimal problem; hence there exists the additional normalization constraint described by Eq. (2) on the control inputs. (The development extends in a natural way to the energy-optimal and fuel-optimal criteria.) The following three definitions establish the concept of the (time-optimal) degree of control spillover.

Definition 7. A state $x_r(T)$, in the subspace $\mathscr{R}^r$ of residual modes governed by Eq. (129), is said to be *reachable in time* T from the state $x_r(0) = 0$ *if there exists a control* $u(t)$, $t \in [0, T]$, $|u_i(t)| \leqslant 1$, $i = 1, 2, \ldots, m$, *such that*

$$x_r(T) = e^{A_r T} \int_0^T e^{-A_r t} B_r u(t)\, dt. \tag{130}$$

Definition 8. The *set of reachable states for time* T is the set S of all states $x_r(T)$ satisfying Eq. (130) for controls satisfying $|u_i(t)| \leqslant 1$.

Definition 9. The *degree of control spillover for time* T of the residual system, Eq. (12) is defined as $\sigma = \sup ||x_r(T)|| \;\forall\; x_r(T) \in S$.

The set of reachable states therefore includes all disturbed states in the residual system subspace attainable in time T when the specified bounded controls are used. The (time-optimal) degree of control spillover is a scalar measure of the magnitude of that set, chosen as the maximum distance to the boundary of that set so as to complement the definition of the (time-optimal) degree of controllability.

Our attention may now be turned toward computing at least an approximation to σ. Recognizing the similarity between definitions 8 and 9 and definitions 1 and 2, we will wish to follow closely the approximation techniques of Ref. 8. The first step is to construct an approximation to S. Assuming for the present that A_r has distinct eigenvalues, we establish the following representation of S.

Lemma 1. Let A_r have distinct eigenvalues $\lambda_1, \lambda_2, \ldots, \lambda_r$, with associated right and left eigenvectors being the column vectors $P_r = [p_1\ p_2 \ldots p_r]$ and $Q_r = [q_1\ q_2 \ldots q_r]$, where $Q_r^T = P_r^{-1}$. Then the residual state $x_r(t) = \delta_r$ which is reached from the origin when the control $u(t)$ is implemented is given by

$$\delta_r = \sum_{k=1}^{r} p_k \int_0^T e^{\lambda_k \tau} q_k^T B u(T - \tau)\, d\tau. \tag{131}$$

Proof. From Eq. (130), we may write

$$\delta_r = x_r(T) = \int_0^T e^{A_r(T-t)} B_r u(t)\, dt. \tag{132}$$

The change of variables $\tau = T - t$ leads to

$$\delta_r = \int_0^T e^{A_r \tau} B_r u(T - \tau)\, dt. \tag{133}$$

Recognizing that $e^{A_r \tau} = P_r e^{\Lambda_r \tau} P_r^{-1}$, where $\Lambda_r = \text{diag}\,[\lambda_1 \ldots \lambda_r]$, we obtain Eq. (131) after partitioning matrices. ■

We define C to be the set of k for which λ_k is real, and we define C^* to be the set obtained by taking one value of k associated with each pair of complex conjugate eigenvalues. Also, we decompose the right and left complex eigenvectors into $p_k = p_k^R + ip_k^I$, $q_k = q_k^R + iq_k^I$ for $k \in C^*$. The following theorem establishes a parallelepiped approximation to S, which is analogous to the approximate recovery region of Ref. 8.

Theorem 2. Let A_r have distinct eigenvalues $\lambda_1, \lambda_2, \ldots, \lambda_r$. The set of reachable states S of the residual-mode system, Eq. (129), can be approximated by the superscribed parallelepiped

$$\delta^* = \{\xi | \xi = \sum_{i=1}^{r} c_i \nu_i, \ \forall\, c_i \ni |c_i| < 1\}, \tag{134}$$

where the set of vectors ν_i, $i = 1, 2, \ldots, r$ comprises the r vectors given by

$$\left(\sum_{\beta=1}^{m} \int_0^T |f_{k\beta}|\, dt\right) p_k, \quad k \in C, \tag{135}$$

$$2\left(\sum_{\beta=1}^{m} \int_0^T \mathrm{Re}|f_{k\beta}|\, dt\right) p_k^R, \quad k \in C^*, \tag{136}$$

$$2\left(\sum_{\beta=1}^{m} \int_0^T \mathrm{Im}|f_{k\beta}|\, dt\right) p_k^I, \quad k \in C^*, \tag{137}$$

where

$$f_{k\beta} = e^{\lambda_k t} q_k^T b \tag{138}$$

and

$$B_r = [b_1 b_2 \ldots b_m]. \tag{139}$$

In Eqs. (136) and (137) Re and Im denote real and imaginary parts respectively. Further, the approximate set S^* is such that at least one point on every face of the parallelepiped is contained in S.

The proof of theorem 2 follows directly from the proof of theorem 1 of Ref. 8 and therefore will not be detailed here.

Our next step is to compute, as an approximation to σ, the maximum distance to the boundary of S^*. This quantity is necessarily the distance to the extremal vertex of the parallelepiped, and we recognize that its value is simply the magnitude of the vector sum of the absolute values of the components of the ν_i. That is,

$$\sigma^* = \sqrt{\sum_{i=1}^{r} \left[\sum_{j=1}^{r} |\nu_{ij}|\right]^2}. \tag{140}$$

We notice immediately that, unlike the approximate degree of controllability (as developed in Ref. 8), the computation of the approximate degree of control spillover does not require a matrix inversion. In addition, since the set of reachable states S is contained within the approximation S^*, the approximate degree of control spillover σ^* is an upper bound to σ and therefore may be regarded as conservative (since our objective will be to keep σ small). It follows that the development of a lower bound to σ (the analog of which was developed in section 3) is unnecessary. Further, we need not concern ourselves with the behavior of the approximation as the set of reachable states becomes dimensionally deficient, because our only concern now is that the approximation always be nonzero when control spillover exists. This condition is satisfied implicitly, since σ^* is an upper bound.

Finally, we note that the preceding development has focused on the time-optimal control problem; therefore, definition 9 establishes a *time-optimal* degree of control spillover. By paralleling the preceding work, we may also develop fuel-optimal and energy-optimal versions of the degree of control spillover. The result is particularly attractive in the energy-optimal case, where the maximum distance to the boundary of the set of reachable states may be computed directly from the maximum eigenvalue of the Gramian of the residual system. In this case, no approximation would be required.

5.3 A Composite Optimization Criterion for Actuator Placement

For use of this measure of control spillover in conjunction with the degree of controllability to optimize actuator placement, the following composite optimization criterion is proposed:

$$\min_{p_j} (\rho^* - \alpha\sigma^*), \tag{141}$$

where α is an adjustable parameter assignable by the design engineer. Here ρ^* may be any of the approximations of ρ which have been cited thus far in this work.

In particular, it will be instructive to consider application of the composite criterion to the example problem of section 4: Hence an examination of the form of the approximation σ^* for an oscillatory system is warranted. We consider a system of undamped harmonic residual modes described by

$$\ddot{\bar{\eta}}_j(t) + \bar{\omega}_j^2\bar{\eta}_j(t) = \bar{\Gamma}_j^T u(t), \quad j = 1, 2, \ldots, r, \tag{142}$$

where the overbars distinguish the residual system from the controlled system described by Eq. (121). The first-order representation of Eq. (142) may be obtained via the substitutions

$$x_{2j-1} = \bar{\eta}_j/\bar{N}_j, \quad x_{2j} = \dot{\bar{\eta}}_j/\bar{N}_j\bar{\omega}_j, \tag{143}$$

so that

$$\begin{bmatrix}\dot{x}_{2j-1}\\ \dot{x}_{2j}\end{bmatrix} = \begin{bmatrix}0 & \bar{\omega}_j\\ -\bar{\omega}_j & 0\end{bmatrix}\begin{bmatrix}x_{2j-1}\\ x_{2j}\end{bmatrix} + \begin{bmatrix}0\\ \bar{\Gamma}_j^T/\bar{N}_j\bar{\omega}_j\end{bmatrix}u. \tag{144}$$

In Eqs. (143) we have followed the normalization of modes which was used to develop the form of the approximate degree of controllability given in Eq. (122). The right and left eigenvectors of the system described by Eq. (144) are the columns of P_r = block diag$[P_j]$ and Q_r = block diag$[Q_j]$, where

$$P_j = \begin{bmatrix}1 & 1\\ i & -i\end{bmatrix}, \quad Q_j = 1/2\begin{bmatrix}1 & 1\\ -i & i\end{bmatrix}. \tag{145}$$

The associated eigenvalues are $\lambda_{2j-1} = i\omega$, $\lambda_{2j} = -i\omega$. Following theorem 2, the set C is empty, and the set C^* contains one entry for each mode j of the system, resulting in one vector v_i each from Eqs. (136) and (137) for each mode. Evaluating Eq. (138) and substituting into Eqs. (136) and (137), we find that these vectors are

$$\sum_{\beta=1}^{m} |\bar{\Gamma}_{j\beta}/\bar{N}_j\bar{\omega}_j| \int_0^T |\sin \bar{\omega}_j t|\, dt \begin{bmatrix}1\\ 0\end{bmatrix}, \tag{146}$$

$$\sum_{\beta=1}^{m} |\bar{\Gamma}_{j\beta}/\bar{N}_j\bar{\omega}_j| \int_0^T |\cos \bar{\omega}_j t|\, dt \begin{bmatrix}0\\ -1\end{bmatrix}. \tag{147}$$

For a final time T which is large compared with the period of the lowest frequency oscillator, these integrals may be replaced by $2/\pi$, their average over a period. With this second approximation, we may replace Eq. (140) with

$$\bar{\sigma} = \frac{2T}{\pi}\sqrt{\sum_{j=1}^{r}\left[\frac{1}{\bar{\omega}_j\bar{N}_j}\,||\bar{\Gamma}_j||_1\right]^2}, \tag{148}$$

where, as in Eq. (122), $||\ldots||_1$ denotes the L_1 norm (the sum of the absolute values of the elements of $\bar{\Gamma}_j$). In the spirit of Eq. (141), the new composite criterion may be written

$$\min_{p_k} (\bar{\rho} - \alpha\bar{\sigma}). \tag{149}$$

This criterion may be applied to the actuator-placement problem of the preceding section with both predictable and interesting results. The simplest version of the problem may be stated: optimally

place one actuator to control the first mode and suppress the interaction of the controller with the second mode of the system. The reassuring result, which is independent both of the modal weights N_1 and $\bar{N}_1$ and of the adjustable parameter α, is to locate the actuator at 0.5. For this location, not only is the degree of controllability maximized, but the degree of control spillover is zero as well.

We could proceed through all the various problems of the previous section and examine the impact of the new composite criterion on each. However, the following two particular cases serve well to illustrate several important points. The first case is to add the fourth system mode as a residual mode to the problem of three controlled modes and two actuators. Under the assumption of balanced modal weights, we know that the optimal solution for $\alpha = 0$ is the actuator location pair (0.2,0.6). As α is increased, this remains the optimal solution through $\alpha = 0.08$. In the range $0.08 < \alpha < 0.09$ there is a discontinuity in the optimal solution, and for $\alpha \geq 0.09$ the optimal set is the pair (0.25,0.75). For this problem, then, we find that the degree of control spillover has not influenced the optimal solution at all until it is weighted heavily enough to cause the actuators to be optimally located at the nodes of the residual mode.

By changing the problem to include both the fourth and fifth modes as residual modes, we intended to preclude the possibility of placing actuators such that the degree of control spillover would be zero. Once more assuming balanced modal weights, we find that the optimal solution for $\alpha = 0$ is again (0.2,0.6). As α increases, this remains the optimal solution until a discontinuous jump occurs in the range $0.9 < \alpha < 1.0$. For $\alpha \geq 1.0$, the optimal locations for the actuator pair is (0.0,1.0)—a design for which the system is uncontrollable! Closer examination of this result reveals that at the discontinuity, α becomes large enough to preclude the possibility of any set of actuator locations which would yield a positive value of the composite criterion, Eq. (149). A value of zero for the criterion was therefore maximal, and the optimization dictated an uncontrollable design.

The obvious conclusion is that the design engineer must exercise some judgment in not placing undue importance on suppressing interaction of the control system with the residual modes, lest the optimal design become untenable.

6. ACTUATOR NUMBER AND PLACEMENT FOR INDEPENDENT MODAL SPACE CONTROL

6.1 Introduction

A new control-design technique, known as Independent Modal Space Control (IMSC), briefly mentioned in subsection 4.1, has recently been developed for generating control laws for large-dimensional harmonic systems such as future large flexible spacecraft.[18,31-33] Here, a simple and succinct summary of this method for optimal control problems is first presented, together with a balanced view of the pros and cons of the approach. The main advantage for linear-quadratic problems is that it allows one to solve the Riccati equation as a set of two-by-two Riccati equations and thus allows one to obtain solutions for very large systems. However, to implement the method, one must use one actuator for each mode to be controlled, which totally nullifies the stated advantage. Here, a new formulation of IMSC is developed which eliminates this restriction and allows one to use a reduced number of actuators by synthesizing an approximation to the optimal feedback which is itself optimal with respect to a modified cost functional.

Another characteristic which distinguishes this method from the standard linear-quadratic design approach is that the control laws are generated without regard to the locations of the actuators. This result has led to the claim that the actuator locations are "immaterial" when IMSC is used.[32] Since a premise of the present work is that actuator placement is of *prime* importance in the control of distributed parameter systems, this claim warrants careful consideration. It is found here that the actuator locations do influence the ultimate physical realization of the control laws as generated by IMSC and therefore must be carefully chosen to assure a physically realizable control (for example, one which is

within the physical limits of the control hardware). Methods for optimization of actuator placement are developed for use in conjunction with IMSC, and the resulting task of actuator placement in some cases can be decoupled from the task of control-law design (a feature unique to IMSC). Finally, the problem of control spillover, addressed in detail in section 5, is here considered in the context of IMSC.

6.2 Summary and Discussion of IMSC

We present in this subsection a concise statement of the IMSC method distilled from Refs. 18, 31, 32, and 33 and compare the method to the more standard linear-quadratic approach. Optimal control of a distributed-parameter system via IMSC is accomplished by first approximating the partial-differential-equation model by a finite set of ordinary differential equations, which for Refs. 18 and 33 take the form

$$M\ddot{q}(t) + Kq(t) = F(t), \quad M > 0, \quad K > 0, \tag{150}$$

where $F(t)$ is a generalized force vector. References 31 and 32 apply IMSC to undamped gyroscopically coupled systems. The approach will be generalized here to handle damped nongyroscopic systems including rigid-body modes.

A transformation matrix P satisfying $P^TMP = I$ and $P^TKP = \Omega = \text{diag}(\omega_1^2, \ldots, \omega_n^2)$ produces the *modal-space representation*

$$\ddot{\nu}_r(t) + \omega_r^2\nu_r(t) = f_r(t), \quad r = 1, 2, \ldots, n, \tag{151}$$

$$\nu(t) = [\nu_1(t) \ldots \nu_n(t)]^T = P^Tq(t), \tag{152}$$

$$f(t) = [f_1(t) \ldots f_n(t)]^T = P^TF(t). \tag{153}$$

A corresponding *state-space representation* of the system is

$$\dot{x}(t) = Ax(t) + W(t), \tag{154}$$

$$x(t) = [x_1(t) \ldots x_{2n}(t)]^T, \tag{155}$$

$$x_{2r-1}(t) = \nu_r(t), \quad x_{2r}(t) = \dot{\nu}_r(t)/\omega, \tag{156}$$

$$W(t) = [W_1^T(t) \ldots W_n^T(t)]^T, \tag{157}$$

$$W_r(t) = [0 \; f_r(t)/\omega_r]^T, \tag{158}$$

$$A = \text{diag}(A_1, \ldots, A_n), \quad A_r = \begin{bmatrix} 0 & \omega_r \\ -\omega_r & 0 \end{bmatrix}. \tag{159}$$

This representation can be put into a more standard form

$$\dot{x}(t) = Ax(t) + Bu(t) \tag{160}$$

by expressing the driving term in Eq. (154) in terms of the actual control inputs $u(t)$ rather than the generalized forces $W(t)$. B takes the form

$$B = [B_1^T \ldots B_n^T]^T, \tag{161}$$

$$B_r = \begin{bmatrix} 0 & \ldots & 0 \\ \phi_r(p_1)/\omega_r & \ldots & \phi_r(p_m)/\omega_r \end{bmatrix}, \tag{162}$$

where $\phi_r(p_i)$ is the rth mode-shape function evaluated at position p_i when the associated actuator is a force actuator and is the spatial derivative of that mode-shape function when the associated actuator is a torque actuator.

The usual linear-quadratic result uses Eq. (160) and the cost functional

$$J = \int_0^T (x^TQx + u^TRu)\, dt, \quad Q \geq 0, \quad R > 0, \tag{163}$$

to obtain

$$u(t) = -R^{-1}B^TK(t)x(t), \tag{164}$$

$$\dot{K}(t) = -KA - A^TK + KBR^{-1}B^TK - Q. \tag{165}$$

It is apparent from Eq. (165) that the actuator-location information, inherent in B, influences the optimal control law described by Eq. (164).

In contrast, IMSC uses Eq. (154) and an alternative cost functional

$$J_{\text{IMSC}} = \int_0^T (x^TQ_{\text{IMSC}}x + W^TR_{\text{IMSC}}W)\, dt, \tag{166}$$

$$Q_{\text{IMSC}} = \text{diag}[Q_1, \ldots, Q_n], \tag{167a}$$

$$R_{\text{IMSC}} = \text{diag}[R_1, \ldots, R_n], \tag{167b}$$

with Q_r and R_r two-by-two matrices associated with each mode. By defining $w_r = [x_{2r-1}\ x_{2r}]^T$, we can decompose the problem into a set of n second-order decoupled optimal control problems as follows:

$$J_{\text{IMSC}} = \sum_{r=1}^{n} J_r = \sum_{r=1}^{n} \int_0^T (w_r^TQ_rw_r + W_r^TR_rW_r)\, dt \tag{168}$$

$$W_r(t) = -R_r^{-1}K_r(t)w_r(t), \tag{169}$$

$$\dot{K}_r(t) = -K_rA_r - A_r^TK_r + K_rR_r^{-1}K_r - Q_r. \tag{170}$$

Here, the generalized controls $W_r(t)$ have been determined independently and in the modal space, which explains the name Independent Modal Space Control. It remains to determine actuator commands u_i that can realize these generalized forces. We will address this later.

Since the feedback solution, Eq. (169), must yield a generalized force vector of the form specified in Eq. (158), a further restriction on R_{IMSC} is imposed. Expanding the second term in the integral of Eq. (168) gives $W_r^TR_rW_r = (f_r(t)/\omega_r)^2\ [R_r]_{22}$, from which we can see that only the element $[R_r]_{22}$ influences the cost functional. The form of $W_r(t)$ in Eq. (158) can be obtained by requiring the first row of R_r^{-1} of Eq. (169) to be zero, and by symmetry the remaining off-diagonal element is zero. If this is written $R_r^{-1} = \text{diag}(0,\ 1/\rho_r)$, then the required form for the original weighting matrix is

$$R_r = \text{diag}(\infty,\ \rho_r). \tag{171}$$

(The alternative of requiring the first row of $R_r^{-1}K_r$ to be zero can allow more freedom in R_r at the expense of freedom in Q_r.)

The preceding summary establishes the foundation for a comparison of the IMSC and standard linear quadratic approaches, and this is given in the following five remarks.

Remark 1. The IMSC approach has a significantly smaller computational requirement, since it requires the solution of n decoupled two-by-two Riccati equations, Eq. (170), rather than a single $2n \times 2n$ Riccati equation, Eq. (165). In fact, an analytical solution of the two-by-two Riccati equation is given in Ref. 32 for the special case of an infinite-time problem, Q_r the identity matrix, and A_r as in Eq. (159).

We can generalize this result to handle arbitrary Q_r and A_r matrices, so that modal damping and rigid-body modes can be included in the system equations, Eq. (150). Without loss of generality, we can choose the state vector to produce the companion form for A_r, since a coordinate transformation is easily accounted for in the choice of Q_r. No transformation of R_r is required, since it weights a scalar generalized control function $f_r(t)$. Then the elements of K_r are given in terms of roots of the two quadratic equations in the following sequence of equations:

$$A_r = \begin{bmatrix} 0 & 1 \\ -a_{21} & -a_{22} \end{bmatrix}, \tag{172}$$

$$k_{12}^2 + 2a_{21}\rho_r k_{12} - q_{11}\rho_r = 0, \tag{173}$$

$$k_{22}^2 + 2a_{22}\rho_r k_{22} - q_{22}\rho_r - 2\rho_r k_{12} = 0, \tag{174}$$

$$k_{11} = k_{12}k_{22}/\rho_r + a_{21}k_{22} + a_{22}k_{12} - q_{12}. \tag{175}$$

Here q_{11}, q_{12}, and q_{22} are the elements of Q_r, and the sign ambiguities in taking the roots of Eqs. (173) and (174) are resolved by the conditions for positive definiteness of K_r, that is, $k_{11} > 0$, $k_{22} > 0$, and $k_{11}k_{22} - k_{12}^2 > 0$.

This generalization of the analytic Riccati solution for A_r in companion form, rather than the skew-symmetric Eq. (159), requires modification of the form of the remaining equations of the original development. Specifically, the choice of state coordinates in Eq. (156) will be simply ν_r and $\dot{\nu}_r$, and similarly the partition of $W_r(t)$ in Eq. (158) becomes $[0\ f_r(t)]^T$. For flexible modes of the system, the nonzero elements of B_r are simply $\phi_r(p_i)$; for rigid-body rotational modes, the nonzero elements of B_r are constants for torque actuators and linear functions of position for force actuators. With these changes, the generalization carries through to all our subsequent results. We return to the restricted form expressed by Eqs. (156) through (162) for the remainder of our results, however, to facilitate further discussion and comparison with the original development.

Remark 2. The physical significance of the weighting matrices R in Eq. (163) and R_{IMSC} in Eqs. (166) are different. If R is diagonal, it weights the relative importance of equal-magnitude inputs $u_i(t)$. By contrast, weights ρ_r of Eq. (171) give the relative importance of equal magnitudes of the generalized forces $f_r(t)/\omega_r$ and have no direct influence on the magnitude of the individual control inputs $u_i(t)$. In fact, the identical control solution can be obtained by absorbing the ρ_r into the corresponding Q_r in each J_r of Eq. (168) and replacing element $[R_r]_{22}$ with unity for all r. With this change it is then clear that the *only* effect of ρ_r was to weight the relative importance of controlling the rth mode, but this is the designer's objective in specifying Q_r.

Remark 3. Examination of the decoupled Riccati equations, Eq. (170), and their associated feedback control laws, Eq. (169), shows that the actuator-location information, inherent in B alone, has no influence on the IMSC optimal-control solution. The actuator locations can therefore be chosen based on any desired criterion, and this becomes an independent design step. This decoupling of the actuator-placement problem and the optimal-control problem is attractive computationally but is not made without some loss of "optimality."

Remark 4. Since the optimal control solution for IMSC is found in the modal space, there exists an extra step of synthesizing this solution in terms of actual control inputs u. From Eqs. (154) and (160), $W(t) = Bu(t)$, but this expression cannot be inverted directly to obtain $u(t)$. The structure of W and B of Eqs. (157), (158), (161), and (162) leads to an equivalent relation:

$$f(t) = B'u(t) = \begin{bmatrix} \phi_1(p_1) & \cdots & \phi_1(p_m) \\ \cdots & \cdots & \cdots \\ \phi_n(p_1) & \cdots & \phi_n(p_m) \end{bmatrix} u(t). \tag{176}$$

The solution of Eq. (176) for $u(t)$ in terms of $f(t)$ requires inversion of matrix B'. This leads to the fundamental limitation of IMSC: the requirement that the number of actuators equal the number of modes in the model ($m = n$), a necessary condition for the existence of $(B')^{-1}$.

Remark 5. The fundamental property of IMSC is that generalized control functions $f(t)$ are designed for the system represented by Eq. (151). The method therefore is not limited to the linear-quadratic optimal-control implementation. In Ref. 33, a pole-placement design technique is developed in terms of IMSC, resulting in an attractive analytic control design.

In the next subsection, a technique is developed by which IMSC may be enhanced to alleviate the stringent requirement on the number of actuators, through the use of a modified cost functional. Then, for the first time, a clear concise explanation of the importance of actuator placement in IMSC is presented. This leads to the development of both open-loop and closed-loop approaches to actuator-location optimization. With the decoupling noted in remark 3, these algorithms can form an independent step in the design of the control system.

6.3 Reduction in the Number of Actuators

The principal disadvantage of IMSC is the requirement that the number of actuators equal the number of modes in the control-system model. This requirement completely nullifies, for practical purposes, the advantage that extremely-large-order Riccati equations can be handled by this design technique. In the design process there would also most likely be a management distaste for letting a computational tool dictate the hardware design (the number of actuators), especially since the hardware configuration is usually frozen in the design evolution long before the system software. Thus, this subsection is devoted to eliminating this stringent restriction on the number of actuators.

Adopting the point of view suggested in remark 2 that each ρ_r should be set to unity, we can write the cost functional in terms of W as

$$J'_{\mathrm{IMSC}} = \int_0^T (x^T Q' x + W^T R' W)\, dt, \tag{177}$$

$$Q' = \mathrm{diag}(Q_1/\rho_1, \ldots, Q_n/\rho_n), \tag{178a}$$

$$R' = \mathrm{diag}(\infty, 1, \ldots, \infty, 1), \tag{178b}$$

and the associated physical control $u(t)$ is to satisfy

$$W(t) = Bu(t). \tag{179}$$

When the number of actuators is less than the number of modes ($m < n$), there will generically be no $u(t)$ which can produce the optimal $W(t)$.

Consider the least-square approximate solution to Eq. (179) given by

$$\bar{u}(t) = B^{\dagger} W(t), \tag{180}$$

$$B^{\dagger} = (B^T B)^{-1} B^T. \tag{181}$$

(Reference 33 dismisses this use of a pseudo-inverse, since it generically will not yield an exact realization of the generalized control $W(t)$.) Recalling Eq. (169), we may write the feedback control which results from this approximate realization of $W(t)$ as

$$\bar{u}(t) = -B^{\dagger}(R')^{-1} K' x(t) = -\bar{G} x(t), \tag{182}$$

where $K' = \mathrm{diag}[K'_1, \ldots, K'_n]$ is the composite matrix of solutions to the Riccati equations, Eq. (170), with Q_r and R_r dictated by Eqs. (178).

It remains to characterize the nature of this feedback control law which is suboptimal with respect to the original cost functional, Eq. (177). The task of identifying the performance index or set of indices for which a given feedback system is optimal is known as the inverse problem of linear optimal control.[34-35] Before applying the various techniques of the inverse problem to generate performance indices for which the feedback system described by Eqs. (160) and (182) is optimal, it will be useful to state several of the general results of the inverse problem.

Consider a general feedback system defined over the finite interval (t_0, t_1) by the equations

$$\dot{x}(t) = A(t)x(t) + B(t)u(t), \tag{183}$$

$$u(t) = -G(t)x(t). \tag{184}$$

Theorem 3. Every system which can be represented in the form of Eqs. (183) and (184) is optimal with respect to some performance functional in the form

$$J = x^T(t_1)Fx(t_1) + \int_{t_0}^{t_1} [x^TQ(t)x + 2u^TS(t)x + u^TR(t)u]\, dt, \tag{185}$$

where Q, R, and F are symmetric and R is positive definite. (The proof is trivial and may be found in Ref. 34.)

From the standard linear-quadratic problem with a crossterm in the cost functional, $G(t)$ in Eq. (184) satisfies

$$G = R^{-1}(S + B^TK), \tag{186}$$

$$\dot{K} = -KA - A^TK + (KB + S^T)R^{-1}(S + B^TK) - Q, \quad K(t_1) = F. \tag{187}$$

It will be useful to observe that the Riccati equation, Eq. (187), may be expressed in terms of G as

$$\dot{K} = -KA - A^TK + G^TRG - Q. \tag{188}$$

Surprisingly, theorem 3 does not require that Q be positive semidefinite; hence the feedback control, Eq. (184), may be destabilizing and yet still be optimal with respect to Eq. (185). Clearly, for the control of large space structures we desire the feedback control, Eq. (182), to be stabilizing; therefore, it must be verified independently that the closed-loop system $(A + B\bar{G})$ is stable.

The solution to the inverse problem is not in general unique, and several methods exist for generating matrices Q, R, S, and F which represent solutions. Here, we will present just two methods, drawn from Refs. 36 and 34 respectively, which separately address the infinite-time and finite-time problems.

Method A. For the specific problem $(t_0,t_1) = (0,\infty)$ with A, B, and G invariant and $(A + BG)$ asymptotically stable, a solution in the form of Eq. (185) to the inverse problem described by Eqs. (183) and (184) may be obtained as follows:

1. Choose a symmetric positive-definite matrix R arbitrarily.
2. Choose a symmetric matrix K arbitrarily.
3. Derive S using Eq. (186): $S = RG - B^TK$.
4. Derive Q from the algebraic form of Eq. (188): $Q = -KA - A^TK + G^TRG$.

For the more general time-varying finite-terminal-time problem, the following method is sufficient to generate a solution.

Method B

1. Let G_0 be any matrix, equivalent in dimension to G, such that, for all $t \in [t_0,t_1]$, (a) G_0B has m linearly independent real eigenvectors and nonpositive eigenvalues, and (b) rank G_0B = rank G_0 = rank B. (Choosing $G_0 = B^TP$ for any real symmetric $P < 0$ will satisfy (a) and (b).)
2. Any pair of symmetric positive-definite matrices R and K which satisfy $G_0 = -R^{-1}B^TK$ will lead to a solution of the inverse problem. (Choosing $R = I$, in particular, will yield $K = -P$.)
3. Q may then be obtained from $\dot{K} = -KA - A^TK + G^TRG - Q$ and F from $F = K(t_1)$.
4. Finally, from Eq. (186), S is given by $S = R(G + G_0)$.

Using either method A or method B, we may now return to the problem at hand and construct, for any stabilizing feedback control law in the form of Eq. (182), a performance index in the form of Eq. (186) for which the control is optimal. In each of the infinite-time and finite-time cases, one specific choice of matrices yields a particularly simple representation of the resulting matrices. Denoting by overbars this specific solution, we may proceed as follows.

Following method A, we select $\bar{R}$, the control weighting matrix for our new cost functional, Eq. (185), as

$$\bar{R} = B^T R' B. \tag{189}$$

Recalling Eq. (179), we note that this is the same control penalty that appears in the original cost functional. We next choose

$$\bar{K} = K'. \tag{190}$$

Substituting Eqs. (182) and (189) into the expression in step 3, we obtain the crossterm

$$\bar{S} = (B^T R' B) B^\dagger (R')^{-1} K' - B^T K'. \tag{191}$$

We may simplify this expression by first noting that the special structure of R' and B leads to the identities

$$B^T R' = B^T (R')^{-1} = B^T. \tag{192}$$

Using Eq. (192), and expanding the pseudo-inverse according to Eq. (181), we obtain

$$\bar{S} = B^T B (B^T B)^{-1} B^T (R')^{-1} K' - B^T K' = B^T K' - B^T K' = 0. \tag{193}$$

Finally, we generate our new state penalty $\bar{Q}$ according to step 4:

$$\bar{Q} = - K'A - A^T K' + K'(R')^{-1} B^{\dagger T} B^T (R')^{-1} K', \tag{194}$$

where again we have used the identities in Eq. (192). Recalling that our original state penalty Q' satisfies

$$Q' = - K'A - A^T K' + K'(R')^{-1} K', \tag{195}$$

we may write

$$\bar{Q} = Q' + K'(R')^{-1} (B^{\dagger T} B^T - I) K'. \tag{196}$$

The feedback control law, Eq. (182), is therefore optimal with respect to a modified cost functional in which only the state weighting matrix has changed. In addition, we note that this particular solution to the inverse problem (defined by Eqs. (189), (193), and (196)) reduces to the original problem if $(B')^{-1}$ exists.

A similar result may be obtained using method B for the time-varying, finite-terminal-time problem. In step 1, we choose

$$G_0 = -B^\dagger K'(t), \tag{197}$$

where $K'(t)$ is the block-diagonal positive-definite solution to the differential Riccati equation of the original problem. It is simple to show that conditions (a) and (b) in step 1 are satisfied by Eq. (197). One possible solution to $G_0 = -(\bar{R})^{-1} B^T \bar{K}$ is then

$$\bar{R} = B^T B, \tag{198}$$

$$\bar{K} = K'. \tag{199}$$

Paralleling the procedure used in the infinite-time problem, we obtain the new state penalty $\bar{Q}$ in terms of the original penalty Q':

$$\bar{Q} = Q' + K'(R')^{-1}(B'^{T}B^{T} - I)K'. \tag{200}$$

This equation is identical in form to Eq. (196), although $\bar{Q}$ is now a function of time. Further, we have $F = K'(T) = 0$ and, from step 4,

$$\bar{S} = \bar{R}(\bar{G} + G_0) = 0, \tag{201}$$

where we have used the identities of Eq. (192) one final time.

In general then, we may state that one performance index for which the feedback control, Eq. (182), is optimal is

$$\bar{J}_{\text{IMSC}} = \int_0^T (x^T\bar{Q}x + W^TR'W)\,dt, \tag{202}$$

with $\bar{Q}$ being defined by Eq. (200).

Remark 6. Reflecting on the form of Eq. (202), we recognize that the $\bar{u}$ given by Eq. (182) is that control among all possible realizable controls which minimizes a modified cost functional in which only the state penalty has changed. As in the original IMSC formulation, the control penalty term is entirely prespecified, and the structure of the state penalty is restricted. Thus, the limited design freedom available in the original formulation remains, since the diagonal blocks of Q' are still assignable by the designer. There is a loss of transparency in the design, however, since now the influence of the assignable elements of Q' on the state performance is not straightforward.

Remark 7. The method proposed here using $\bar{u}$ allows one to compute optimal control laws (relative to $\bar{J}_{\text{IMSC}}$) for systems of arbitrarily large dimension, thus allowing all the modal information one has about the system to be considered. Further, no specific requirement is placed on the number of actuators, although we must require that the feedback gain $\bar{G}$ stabilize the system. There is no need for truncation in the control-law design, since the computation of the Riccati-equation solution from the analytical expressions, Eqs. (173), (174), and (175), and the computation of the control $\bar{u}$, Eq. (180), requiring the inverse of an m-by-m matrix, can both be performed for extremely large systems. The limiting computation is the conversion of Eq. (150) to the form of Eq. (151) to determine the mode shapes and frequencies.

Remark 8. It follows directly that control spillover can be eliminated by use of the new extended IMSC approach. Observation spillover will still be present, but the total absence of control spillover guarantees stability of the closed-loop system for the given large-order model. The limiting factor here is the fidelity of one's knowledge of higher order modes.

Remark 9. The design of optimal controllers using standard linear-quadratic theory is actually iterative. The designer chooses Q and R matrices, performs simulations to study the resulting performance, and iteratively adjusts the entries in R to prevent saturation of the actuators and the entries in Q to obtain the desired performance. The advantages achieved in general by IMSC are made at the expense of freezing the choice of the control weighting matrix. One no longer has weighting factors with direct one-to-one correspondence to the input magnitudes $\bar{u}_i$, which for conventional design are adjusted to avoid individual actuator saturation. Only the entries in the Q matrix are at the designer's disposal, and these are properly intended for other purposes and do not have a direct relation to any given actuator.

In the next subsection, methods for actuator-location optimization are developed which balance the system to cause the expectations of the commands to each actuator to be of similar magnitude. This can partially offset the lack of adjustment capability in the control penalty matrix.

Remark 10. The advantages of this new formulation of IMSC as described in remarks 7 and 8 are made at the expense of loss of design transparency, as described in remark 6. However, considering the advantages inherent in lifting the stringent requirement on the number of actuators, a designer should be willing to pursue this new approach, provided the resulting closed-loop system is stable. One sufficient condition for stability of the closed-loop system is that $\underline{Q}$ be positive definite.

6.4 Actuator Placement for IMSC

Baruh and Meirovitch[18] state that an advantage of IMSC is that the actuator locations are immaterial, provided $B^{\dagger}$ is not singular. The statement is valid in the sense that, as noted in remark 3, rather than solving for optimal control inputs, IMSC poses a problem which optimizes the generalized forces for each mode without regard for how these forces might be produced by the actuators. However, the determination of the actuator commands depends *fundamentally* on the actuator locations.

Remark 11. The consequences of improperly chosen actuator locations can be disastrous. It is not difficult to generate examples which demonstrate that the force or torque required of a given actuator can grow without bound as the actuator location approaches a position for which the system is uncontrollable.

We now develop methods for optimizing the actuator locations in order to minimize the actual control effort. First, a computationally simple open-loop approach is presented, and then by similar reasoning a more precise closed-loop approach is developed. Finally, a method is given which in addition minimizes residual mode excitation.

Open-Loop Approach to Actuator Placement

The objective in selecting the locations for the actuators is to minimize the control effort $\bar{u}^T\bar{u}$. We define the singular-value decomposition of $B^{\dagger}$ to be $U\Sigma V^T$ with singular values $\sigma_1(B^{\dagger}) > 0, \ldots, \sigma_m(B^{\dagger}) > 0$, assuming that there are no redundant actuators. From Eq. (180)

$$\begin{aligned}\bar{u}^T\bar{u} &= W^T(B^{\dagger})^T(B^{\dagger})W \\ &= (W^TV)\,\mathrm{diag}[\sigma_1^2(B^{\dagger}), \ldots, \sigma_m^2(B^{\dagger})](V^TW).\end{aligned} \tag{203}$$

The matrix V is a unitary transformation which does not change the length of the vector W. If we assume no knowledge of the vectors W that will appear in operation, so that all values of W are equally likely, then the control effort is minimized when the actuator locations p_j are chosen to make the largest $\sigma_i(B^{\dagger})$ as small as possible, or equivalently

$$\max_{p_j}[\min_i \sigma_i(B)]. \tag{204}$$

At this point, if a discrete set of possible actuator locations exists, the set chosen is simply the one which yields the largest minimum singular value. Alternatively, if a gradient search is to be performed over the space of possible actuator locations, the gradient of σ_i with respect to p_j may be developed as

$$\begin{aligned}\frac{\partial\sigma_i}{\partial p_j} &= \eta_i^T \frac{\partial(B^{\dagger})^T(B^{\dagger})}{\partial p_j}\xi_i/(\eta_i^T\xi_i) \\ &= \eta_i^T\left(\frac{\partial B^{\dagger T}}{\partial p_j}B^{\dagger} + B^{\dagger T}\frac{\partial B^{\dagger}}{\partial p_j}\right)\xi_i/(\eta_i^T\xi_i),\end{aligned} \tag{205}$$

where ξ_i and η_i are the columns of V and U respectively and Eq. (204) is evaluated for i associated with the minimum singular value.

Closed-Loop Approach to Actuator Placement

Since f is to be generated as a feedback control, we can obtain information about its magnitude for an ensemble of initial conditions and use this information to improve the preceding technique. We consider the initial conditions to be unknown and assume them to be zero mean and Gaussian with covariance $P_0 = E(x_0 x_0^T)$. Then the actuators are to be placed to minimize the maximum eigenvalue of a control-effort matrix, which for finite-time problems takes the form

$$\mathcal{J} = E \int_0^T \bar{u}\, \bar{u}^T\, dt. \tag{206}$$

For infinite-time problems, the control effort matrix would be the limit of Eq. (206) as $T \to \infty$.

With R' and K' defined as in subsection 6.3, the optimally controlled system, Eq. (154), may be expressed as

$$\dot{x} = [A - (R')^{-1}K']x = \bar{A}x, \tag{207}$$

with the solution

$$x(t) = \Phi(t)x_0. \tag{208}$$

Recalling that $\bar{u}$ may be expressed as

$$\bar{u} = B^* W = -B^*(R')^{-1}K'x, \tag{209}$$

we can write the criterion $\mathcal{J}$ as

$$\mathcal{J} = B^*\{(R')^{-1}[\int_0^T K'\Phi P_0 \Phi^T K'\, dt](R')^{-1}\}B^{*T} \tag{210}$$

$$= B^* \mathcal{P} B^{*T}. \tag{211}$$

Because of the decoupling of the optimal-control calculation from the actuator locations p_j, the optimal trajectory x and the Riccati-equation solution K' are independent of p_j, making the matrix $\mathcal{P}$ defined in Eq. (211) independent of p_j. This vastly simplifies the computations required for optimizing the eigenvalues of $\mathcal{J}$ and makes the approach used here quite reasonable in terms of computational effort. The objective is to obtain

$$\min_{p_j}[\max_i \lambda_i(B^* \mathcal{P} B^{*T})], \tag{212}$$

which can be accomplished as before by using gradient expressions for the eigenvalue derivatives.

In the infinite-time case, $T \to \infty$, the K' matrix becomes time invariant. Letting $P(t) = \Phi(t)P_0\Phi^T(t)$, one can generate $\mathcal{P}$ from

$$\mathcal{P} = (R')^{-1}K'(\int_0^\infty P(t)\, dt)K'(R')^{-1}, \tag{213}$$

where $P(t)$ satisfies

$$dP(t)/dt = \bar{A}P + P\bar{A}. \tag{214}$$

Actuator Placement for Spillover Suppression

In the previous literature on IMSC, the number of modes to be controlled could not exceed the number of actuators, and control spillover questions were potentially quite serious. Reference 18, having adopted the attitude that actuator placement is immaterial for generating the control signals as long as the system is controllable, suggests placing the actuators at nodes of the first residual mode. Actually it is more reasonable to try to suppress the control spillover into a set of residual modes by placement of the actuators, but this placement would be at the expense of minimizing the control effort required to control the controlled modes. Hence a compromise would be called for. As in section 5, we let

$$\dot{x}_r = A_r x_r + B_r \bar{u} \tag{215}$$

represent the set of residual modes not included in the control-system model. Then we wish to keep $B_r \bar{u} = B_r B^* W$ small. In the open-loop approach, we would seek to adjust the actuator locations p_j to obtain

$$\max_{p_j} [\min_i \sigma_i(B) - \alpha_1 \max_k \sigma_k(B_r B^*)], \tag{216}$$

where α_1 is an adjustable parameter. In the closed-loop case we wish to keep

$$E \int_0^T B_r \bar{u}\bar{u}^T B_r^T \, dt \tag{217}$$

small, which leads to the actuator-placement criterion

$$\min_{p_j} [\max_i \lambda_i(B^* \mathcal{P} B^{*T}) + \alpha_2 \max_i \lambda_i(B_r B^* \mathcal{P} B^{*T} B_r^T)]. \tag{218}$$

The added complication of using such a criterion over that of Eq. (212) is negligible. However, the results of the previous subsection eliminated the fundamental shortcoming of IMSC of requiring one actuator for each mode to be controlled, and, as noted in remark 8, this allows us to eliminate the control spillover problem entirely for all known modes. Thus, there is then no need for considering spillover suppression in the choice of actuator locations.

6.5 Summary

A new formulation of the IMSC method has been developed which allows one to pick the number of actuators to use. The analytical solution for the optimal control law is extended to handle modal damping and rigid-body modes. These two results allow one to solve the optimal-control problem for extremely high dimensional systems. The price one pays is that the cost functional no longer contains the usual adjustable parameters which have a one-to-one correspondence to each controller's action and that the state penalty only indirectly dictates the state performance; hence it is more difficult to tune the cost functional to meet the desired performance. Methods of locating the actuators to minimize the control effort are developed, and the methods are found to be comparatively simple because of the decoupling inherent in IMSC which can separate the control-law determination from the actuator-placement problem.

7. CONCLUSIONS

The problem of actuator placement for the control of distributed-parameter systems has been considered in detail, motivated by the general problem of control of large space structures. Significant advances have been made in understanding the utility of the concept of degree of controllability as a criterion for actuator placement. This has been achieved through application to several relatively simple, yet significant, numerical problems. A new method for approximating the degree of controllability has been formulated via discretization of the continuous-time system, providing a conservative (lower-bound) approximation to the exact value. The concept of a degree of control spillover has been introduced to address the acknowledged limitation in the fidelity of finite-dimensional models of distributed-parameter systems. Finally, the problem of number and placement of actuators has been considered in conjunction with a specific nonstandard formulation of linear-quadratic optimal control known as Independent Modal Space Control. A reformulation of the technique, which lifts the restriction on the number of actuators required, along with the development of methods for actuator-placement optimization, adds significantly to the practical utility of the IMSC design technique.

The results of this research suggest several new areas of investigation, with two areas being possibly most significant. The first area involves the difficulties encountered in determining globally optimal solutions for actuator placement on a simple flexible structure, as detailed in section 4. These

difficulties suggest that the standard gradient-based search techniques, as employed here, are inappropriate for general large-dimensional, multiple-input control problems associated with systems such as large flexible spacecraft. The general problem is characterized by a large number of local optima, often with values near the global optimum, by "steep" gradients, and numerical problems associated with the gradient evaluation, and in some cases by the existence of a discrete solution space in the true physical problem. These characteristics occur also in such diverse engineering problems as structural optimization, optimal kinematic synthesis, and optimal allocation of computer resources. In these fields, the use of search strategies based on evolutionary or genetic algorithms and the use of methods of combinatorial heuristics have begun to be applied with some success. The practical application of the actuator-placement criteria discussed herein, to significant engineering design problems, will likely require the implementation of such sophisticated optimization methods.

The second area of investigation which may yield significant results involves extensions of the contributions of section 6 to the IMSC design technique. Although the developments of that section are limited to linear-quadratic optimal control, IMSC itself is not so limited. The newly developed actuator-placement techniques presented here are clearly applicable to other IMSC-based design approaches (particularly pole placement). The application of the new method for lifting the restriction on the number of actuators to other IMSC design strategies, however, is not straightforward and requires careful consideration. The problem that arises in pole placement is that the optimal gains which achieve the desired pole allocation can be only approximately synthesized when the number of actuators is reduced, and the stability of the resulting closed-loop system in the general case has not been assessed. Finally this new formulation of IMSC should be applied to a significant control design problem to determine guidelines with which the practical design engineer may use the technique successfully.

8. REFERENCES

1. R.E. Kalman, "On the General Theory of Control Systems," pp. 481-492 in *Proceedings of the First International Congress on Automatic Control*, Moscow, 1960, Vol. 1.

2. R.E. Kalman, Y.C. Ho, and K.S. Narendra, "Controllability of Linear Dynamical Systems," Contributions to Differential Equations **1** (No. 2), 182-213 (1961).

3. R.G. Brown, "Not Just Observable, But How Observable," pp. 709-714 in *Proceedings of the 1966 National Electronics Conference*, Vol. 22.

4. R.A. Monzingo, "A Note on Sensitivity of System Observability," IEEE Trans. Automatic Control **AC-12**, 314-315 (June 1967).

5. C.D. Johnson, "Optimization of a Certain Quality of Complete Controllability and Observability for Linear Dynamical Systems," ASME Trans. J. Basic Engng. **D 91**, 228-238 (1969).

6. P.C. Müller and H.I. Weber, "Analysis and Optimization of Certain Qualities of Controllability and Observability for Linear Dynamical Systems," Automatica **8**, 237-246 (1972).

7. B. Friedland, "Controllability Index Based on Conditioning Number," ASME Trans. J. Dynamic Systems, Measurement, and Control **97**, 444-445 (Dec. 1975).

8. C.N. Viswanathan, R.W. Longman, and P.W. Likins, "A Definition of the Degree of Controllability—A Criterion for Actuator Placement," pp. 369-384 in *Proceedings of the 2nd VPI&SU/AIAA Symposium on Dynamics and Control of Large Flexible Spacecraft*, June 1979.

9. C.N. Viswanathan, "Aspects of Control of Large Flexible Spacecraft," doctoral dissertation, Columbia University, 1980.

10. C.N. Viswanathan and R.W. Longman, "The Determination of the Degree of Controllability for Dynamic Systems with Repeated Eigenvalues," in *Proceedings of the NCKU/AAS Symposium on Engineering Science and Mechanics*, Tainan, Taiwan, Dec. 1981.

11. R.W. Longman and K.T. Alfriend, "Actuator Placement from Degree of Controllability Criteria for Regular Slewing of Flexible Spacecraft," Acta Astronautica **8** (No. 7), 703-718 (1981).

12. M. Athans and P.L. Falb, *Optimal Control*, McGraw-Hill, 1966.

13. J.-N. Juang and G. Rodriguez, "Formulations and Applications of Large Structure Actuator and Sensor Placements," pp. 247-262 in *Proceedings of the 2nd VPI&SU/AIAA Symposium on Dynamics and Control of Large Flexible Spacecraft*, June 1979.

14. S.E. Aidarous, M.R. Gevers, and M.J. Installé, "Optimal Point-wise Discrete Control and Controllers' Allocation Strategies for Stochastic Distributed Systems," Int. J. Control **24**, 493-508 (1976).

15. J.C.E. Martin, "Optimal Allocation of Actuators for Distributed-Parameter Systems," ASME Trans. J. Dynamic Systems, Measurement, and Control **100**, 227-228 (Sept. 1978).

16. P.C. Hughes and R.E. Skelton, "Controllability and Observability for Flexible Spacecraft," pp. 385-408 in *Proceedings of the 2nd VPI&SU/AIAA Symposium on Dynamics and Control of Large Flexible Spacecraft*, June 1979.

17. B.P. Wang and W.D. Pilkey, "Optimal Damper Location in the Vibration Control of Large Space Structures," pp. 379-392 in *Proceedings of the 3rd VPI&SU/AIAA Symposium on Dynamics and Control of Large Flexible Spacecraft*, June 1981.

18. H. Baruh and L. Meirovitch, "On the Placement of Actuators in the Control of Distributed Parameter Systems," presented as AIAA paper 81-0638 at the 22nd Structures, Structural Dynamics and Materials Conference, April 6-8, 1981.

19. R.E. Skelton and D. Chiu, "Optimal Selection of Inputs and Outputs in Linear Stochastic Systems," in *Proceedings of the NCKU/AAS Symposium on Engineering Science and Mechanics*, Tainan, Taiwan, Dec. 1981.

20. G.J. Kissel and J.G. Lin, "Spillover Prevention via Proper Synthesis/Placement of Actuators and Sensors," pp. 1213-1218 in *Proceedings of the 1982 American Control Conference*, Vol. 3.

21. G. Schulz and G. Heimbold, "Integrated Actuator/Sensor Positioning and Feedback Design for Large Flexible Structures," pp. 476-483 in *Proceedings of the AIAA Guidance and Control Conference*, Aug. 1982.

22. R.A. Laskin, R.W. Longman, and P.W. Likins, "A Definition of the Degree of Controllability for Fuel Optimal Systems," pp. 1-14 in *Proceedings of the 3rd VPI&SU/AIAA Symposium on Dynamics and Control of Large Flexible Spacecraft*, June 1981.

23. R.W. Longman and K.T. Alfriend, "Energy Optimal Degree of Controllability and Observability for Regulator and Maneuver Problems," in *Proceedings of the 16th Annual Conference on Information Sciences and Systems*, Princeton, N.J., Mar. 1982.

24. B.C. Moore, "Principal Component Analysis in Linear Systems: Controllability, Observability and Model Reduction," IEEE Trans. Automatic Control **AC-26** (No. 1), 17-32 (Feb. 1981).

25. A. Arbel and N.K. Gupta, "Optimal Actuator and Sensor Locations in Oscillatory Systems," presented at The 13th Asilomar Conference on Circuits, Systems, and Computers, Nov. 1979.

26. A. Arbel, "Controllability Measures and Actuator Placement in Oscillatory Systems," Int. J. Control **33** (No. 3) 565-574 (1981).

27. W.E. Vander Velde and C.R. Carignan, "Number and Placement of Control System Actuators Considering Possible Failures," pp. 7-15 in *Proceedings of the 1982 American Control Conference*, Vol. 1.

28. L. Meirovitch, *Analytical Methods in Vibrations*, MacMillan, 1967.

29. R.A. Laskin, "Aspects of the Dynamics and Controllability of Large Flexible Structures," doctoral dissertation, Columbia University, 1982.

30. M.J. Balas, "Feedback Control of Flexible Systems," IEEE Trans. Automatic Control **AC-23**, 673-679 (1978).

31. L. Meirovitch, H.F. VanLandingham, and H. Öz, "Distributed Control of Flexible Spinning Spacecraft," J. Guidance and Control **2** (No. 5), 407-415 (1979).

32. H. Öz and L. Meirovitch, "Optimal Modal Space Control of Flexible Gyroscopic Systems," J. Guidance and Control **3** (No. 3) 218-226 (1980).

33. L. Meirovitch, H. Baruh, and H. Öz, "A Comparison of Control Techniques for Large Flexible Systems," presented as AAS paper 81-195 at the 1981 AAS/AIAA Astrodynamics Specialist Conference, Aug. 3-5, 1981.

34. E. Kreindler and A. Jameson, "Optimality of Linear Control Systems," IEEE Trans. Automatic Control **AC-17**, 349-351 (1972).

35. A. Jameson and E. Kreindler, "Inverse Problem of Linear Optimal Control," SIAM J. Control **11** (No. 1), 1-19 (1973).

36. J. Casti, "The Linear Quadratic Control Problem: Some Results and Outstanding Problems," SIAM Review **22** (No. 4) 459-485 (1980).